

**PHYSICAL MODEL SIMULATION OF 3-D SUBSIDENCE
INDUCED BY UNDERGROUND MINES**



Thanittha Thongprapha

**A Thesis Submitted in Partial Fulfillment of the Requirements for the
Degree of Doctor of Philosophy of Engineering in Geotechnology**

Suranaree University of Technology

Academic Year 2014

การจำลองเชิงกายภาพของการทรุดตัวของผิวดินในสามมิติที่เกิดจาก
การทำเหมืองใต้ดิน



นางสาวธนัชฎา ทองประภา

วิทยานิพนธ์นี้เป็นส่วนหนึ่งของการศึกษาตามหลักสูตรปริญญาวิศวกรรมศาสตรดุษฎีบัณฑิต

สาขาวิชาเทคโนโลยีธรณี

มหาวิทยาลัยเทคโนโลยีสุรนารี

ปีการศึกษา 2557

**PHYSICAL MODEL SIMULATION OF 3-D SUBSIDENCE
INDUCED BY UNDERGROUND MINES**

Suranaree University of Technology has approved this thesis submitted in partial fulfillment of the requirements for the Degree of Doctor of Philosophy.

Thesis Examining Committee

(Dr. Decho Phueakphum)

Chairperson

(Prof. Dr. Kittitep Fuenkajorn)

Member (Thesis Advisor)

(Dr. Prachya Tepnarong)

Member

(Dr. Anisong Chitnarin)

Member

(Assoc. Prof. Ladda Wannakao)

Member

(Prof. Dr. Sukit Limpijumnong)

Vice Rector for Academic Affairs
and Innovation

(Assoc. Prof. Flt. Lt. Dr. Kontorn Chamniprasart)

Dean of Institute of Engineering

ชนิษฐา ทองประภา : การจำลองเชิงกายภาพของการทรุดตัวของผิวดินในสามมิติที่เกิดจากการทำเหมืองใต้ดิน (PHYSICAL MODEL SIMULATION OF 3-D SUBSIDENCE INDUCED BY UNDERGROUND MINES) อาจารย์ที่ปรึกษา : ศาสตราจารย์ ดร.กิตติเทพ เพ็ญขจร, 93 หน้า.

การจำลองเชิงกายภาพและเชิงตัวเลขได้ดำเนินการเพื่อศึกษาพื้นผิวดินทรุดตัวที่เกิดจากช่องเหมืองใต้ดินภายใต้สภาวะที่เกินกว่าจุดวิกฤต การศึกษามุ่งเน้นในด้านผลกระทบของรูปร่างทรงเรขาคณิตของช่องเหมือง ความลึก และขนาดก้อนของชั้นหินปิดทับที่มีผลต่อมุมการไหลและการทรุดตัวสูงสุด กรวดก้อนสามขนาด (3, 6 และ 12 มิลลิเมตร) ที่สะอาดและมีความสม่ำเสมอถูกใช้ในการจำลองเป็นก้อนเพื่อแสดงลักษณะของชั้นหินปิดทับ โครงจำลองทางกายภาพได้ถูกนำมาใช้สำหรับการจำลองการทรุดตัวในสามมิติแบบย่อส่วน โดยที่ความกว้างของช่องเหมืองจะถูกกำหนดให้มีค่าคงที่เท่ากับ 5 เซนติเมตร อัตราส่วนระหว่างขนาดก้อนต่อความกว้างของช่องเหมืองผันแปรจาก 0.06, 0.12 ถึง 0.24 อัตราส่วนระหว่างความลึกต่อความกว้างของช่องเหมืองผันแปรจาก 1 ถึง 5 อัตราส่วนระหว่างความสูงต่อความกว้างของช่องเหมืองผันแปรจาก 0.2 ถึง 1 และอัตราส่วนระหว่างความยาวต่อความกว้างของช่องเหมืองผันแปรจาก 1 ถึง 5 ผลการทดสอบระบุว่ามุมการไหลและการทรุดตัวสูงสุดมีค่าลดลงด้วยการเพิ่มขึ้นของอัตราส่วนระหว่างขนาดก้อนต่อความกว้างของช่องเหมือง และมุมการไหลเพิ่มขึ้นตามความสูงและความยาวของช่องเหมือง อัตราส่วนระหว่างการทรุดตัวสูงสุดต่อความกว้างของช่องเหมืองและมุมการไหลจะเริ่มมีค่าคงที่เมื่ออัตราส่วนระหว่างความยาวต่อความกว้างของช่องเหมืองมีค่าเกินกว่า 3 นอกจากนี้ภายใต้รูปร่างของช่องเหมืองที่เหมือนกัน การเพิ่มขึ้นของความลึกของช่องเหมืองส่งผลให้มุมการไหลและการทรุดตัวสูงสุดมีค่าลดลง เนื่องจากการเกิดช่องว่างระหว่างเม็ดกรวดในชั้นหินปิดทับที่อยู่เหนือช่องเหมืองตามความลึกที่เพิ่มขึ้น การศึกษานี้ได้ทำการเปรียบเทียบวิธีการเชิงประจักษ์ที่น่าเสนอโดย Peck และแบบจำลอง PFC^{2D} กับผลการทดสอบเชิงกายภาพ วิธีการเชิงประจักษ์สำหรับวัสดุที่ไม่มีเส้นใยติดซึ่งถูกนำเสนอโดย Rankin และ O'Reilly and New มีความสอดคล้องกันดีกับผลการทดสอบที่ได้จากแบบจำลองเชิงกายภาพ โดยเฉพาะอย่างยิ่งเมื่ออัตราส่วนระหว่างความลึกต่อความกว้างของช่องเหมืองมากกว่า 2 ผลการคำนวณโดยวิธีการเชิงประจักษ์แสดงให้เห็นว่าปริมาณของร่องการทรุดตัวมักจะมีค่าน้อยกว่าปริมาณของช่องเหมืองใต้ดิน นอกจากนี้ผลจากแบบจำลอง PFC^{2D} มีความสอดคล้องเป็นอย่างดีกับผลที่ได้จากแบบจำลองเชิงกายภาพในทุกกรณี ดังนั้นแบบจำลองเชิงคณิตศาสตร์ที่ได้รับการตรวจสอบนี้จึงสามารถใช้ในการประเมินเพื่อทำการ

คาดคะเนพฤติกรรมการทำงานของผิวหนังภายใต้สภาวะที่เกินกว่าจุดวิกฤตของมวลหินที่มีรอยแตกบริเวณเนื้อช่องเหมืองได้



สาขาวิชา เทคโนโลยีธรณี _____

ปีการศึกษา 2557

ลายมือชื่อนักศึกษา _____

ลายมือชื่ออาจารย์ที่ปรึกษา _____

THANITTHA THONGPRAPHA : PHYSICAL MODEL SIMULATION OF
3-D SUBSIDENCE INDUCED BY UNDERGROUND MINES. THESIS
ADVISOR : PROF. KITTITEP FUENKAJORN, Ph.D., P.E., 93 PP.

ANGLE OF DRAW/MAXIMUM SUBSIDENCE/SUBSIDENCE TROUGH/
UNDERGROUND OPENING

Physical and numerical model simulations have been performed to determine the surface subsidence induced by underground opening under super-critical conditions. The study is focus on the effects of opening geometry and depth and block size of the overburden on the angle of draw (γ) and the maximum subsidence (S_{\max}). Clean and uniform granular materials with three different sizes (3, 6 and 12 mm) are used to simulate individual blocks. A trap door apparatus is used to represent the scaled-down three-dimensional simulations. The opening width (W) is maintained constant at 5 cm. The block size-to-width ratio (B_s/W) vary from 0.06, 0.12 to 0.24, opening depth-to-width ratios (Z/W) from 1 to 5, opening height-to-width ratios (H/W) from 0.2 to 1, and opening length-to-width ratios (L/W) from 1 to 5. The results indicate that γ and S_{\max} decrease with increasing B_s/W ratios. The angle of draw increases with opening height (H/W) and length (L/W). The S_{\max}/W ratios and γ approach constants when L/W is beyond 3. Under the same opening geometry, increasing the opening depth results in a reduction of γ and S_{\max} , primarily because new voids has been created in the overburden above the opening when the opening depth increases. The empirical solution given by Peck (1969) and the PFC^{2D} simulation are compared with the physical models. The empirical solutions for

cohesionless material provided by Rankin (1988) and O'Reilly and New (1982) fit well to the physical model results, particularly when Z_r/W greater than 2. It indicates that the trough volume is usually less than the opening volume. The results of PFC^{2D} agree reasonably well with those obtained from the physical models for all cases. These verified numerical models can be extrapolated to predict the super-critical subsidence behavior of fractured rock mass above mine openings.



School of Geotechnology

Academic Year 2014

Student's Signature _____

Advisor's Signature _____

ACKNOWLEDGMENTS

I wish to acknowledge the funding supported by Royal Golden Jubilee Ph.D. scholarship awarded by the Thailand Research Fund under the office of the Prime Minister, the Royal Thai Government.

I would like to express my sincere thanks to Prof. Dr. Kittitep Fuenkajorn for his valuable guidance and efficient supervision. I appreciate his strong support, encouragement, suggestions and comments during the research period. I also would like to express my gratitude to Prof. Dr. Jaak J.K. Daemen for supporting, teaching and advice during my research at University of Nevada, Reno, United States. My heartiness thanks to Dr. Decho Phueakphum, Assoc. Prof. Ladda Wannakao, Dr. Prachya Tepnarong and Dr. Anisong Chitnarin for their constructive advice, valuable suggestions and comments on my research works as thesis committee members. Grateful thanks are given to all staffs of Geomechanics Research Unit, Institute of Engineering who supported my work.

Finally, I would like to thank beloved parents for their love, support and encouragement.

Thanittha Thongprapha

TABLE OF CONTENTS

	Page
ABSTRACT (THAI)	I
ABSTRACT (ENGLISH).....	III
ACKNOWLEDGEMENTS	V
TABLE OF CONTENTS.....	VI
LIST OF TABLES	X
LIST OF FIGURES	XI
SYMBOLS AND ABBREVIATIONS.....	XIV
CHAPTER	
I INTRODUCTION.....	1
1.1 Background and rationale	1
1.2 Research objectives.....	2
1.3 Scope and limitations	2
1.4 Research methodology	3
1.4.1 Literature review.....	5
1.4.2 Sample collection and preparation.....	5
1.4.3 Design and fabrication of the test frame.....	5
1.4.4 Physical model simulation.....	5
1.4.5 Empirical Subsidence Calculations	6

TABLE OF CONTENTS (Continued)

	Page
1.4.6 Computer simulation	6
1.4.7 Analysis and comparisons	6
1.4.8 Discussions and conclusion	6
1.4.9 Thesis writing	6
1.5 Thesis contents	7
II LITERATURE REVIEW	8
2.1 Introduction	8
2.2 Calculation, prediction and monitoring of surface subsidence ..	8
2.2.1 Calculation with profile function method.....	8
2.2.2 Calculation with SALT_SUBSID program	12
2.2.3 Prediction with PFC 2D software	13
2.2.4 The monitoring and prediction of mining subsidence ..	14
2.3 Physical modeling	17
2.4 Empirical subsidence calculations	22
2.5 Computer modeling	23
2.6 Effect of underground opening geometries and overburden properties on surface subsidence	26
2.7 Previous relevant researches	30
III MATERIAL CHARACTERISTICS	35
3.1 Introduction	35

TABLE OF CONTENTS (Continued)

	Page
3.2 Sample preparation	35
3.2.1 Grain size analysis.....	35
3.2.2 Direct shear test.....	38
IV TRAP DOOR APPARATUS.....	44
4.1 Introduction.....	44
4.2 Design and fabrication of the test apparatus	44
V PHYSICAL MODEL SIMULATION	49
5.1 Introduction.....	49
5.2 Physical model testing	49
5.3 Test results	53
VI EMPIRICAL SUBSIDENCE CALCULATION	62
6.1 Introduction.....	62
6.2 Previous studies on settlement trough	62
6.3 Comparisons of subsidence trough profiles.....	64
6.4 Volume of surface settlement	66
VII NUMERICAL ANALYSIS.....	72
7.1 Introduction.....	72
7.2 Discrete element analyses.....	72
7.3 Comparison of numerical and physical models.....	77
VIII DISCUSSIONS AND CONCLUSIONS	82

TABLE OF CONTENTS (Continued)

	Page
8.1 Discussions and conclusions.....	82
8.2 Recommendations for future studies	84
REFERENCES	85
BIOGRAPHY	93



LIST OF TABLES

Table	Page
3.1 Grain size analysis.....	38
3.2 Mechanical properties of tested granular materials.....	43
6.1 Empirical solutions for estimation of settlement trough width.....	65
6.2 Estimation of the settlement trough width using different approaches when $B_s/W = 0.10$, $Z_r/W = 2$, $H/W = 0.5$ and $L/W = 2$	69
7.1 PFC ^{2D} simulation parameters.....	75

LIST OF FIGURES

Figure	Page
1.1 Research methodology.....	4
2.1 Influence of extraction width on subsidence.....	10
2.2 Schematic of ground movements caused by subsidence.....	11
2.3 Small-scale experimental model.....	19
2.4 Classical trap door problem.....	19
2.5 Surface settlement profiles induced by the trap door apparatus.....	21
2.6 Surface subsidence curves of different unconsolidated layers thickness.....	28
2.7 Schematic of the trap door apparatus.....	28
2.8 Graph suggested by NCB.....	32
2.9 Physical model for prediction of subsidence.....	32
2.10 Variables used by Aracheeploha et al. (2009).....	34
3.1 Grain size distribution curves of tested materials.....	36
3.2 Granular materials used to simulate overburden.....	37
3.3 Estimation of roundness and sphericity of sedimentary particles.....	39
3.4 Direct shear device SBEL DR44 used in this study.....	39
3.5 Shear stresses as a function of shear displacement.....	40
3.6 Shear strength as a function of normal stress obtained from direct shear testing.....	41

LIST OF FIGURES (Continued)

Figure	Page
4.1 Trap door apparatus used in this study.....	45
4.2 Perspective view of trap door apparatus.....	46
4.3 Front view of trap door apparatus.....	46
4.4 Side view of trap door apparatus.....	47
4.5 Plan view of trap door apparatus.....	47
4.6 Measurement system of trap door apparatus.....	48
5.1 Variables used in physical model simulations and analysis.....	51
5.2 Example of three-dimensional laser scanned image of surface subsidence.....	52
5.3 Definition of angle of draw.....	54
5.4 Angle of draw as a function of the opening length-to-width ratio.....	55
5.5 Angle of draw as a function of the opening height-to-width ratio.....	56
5.6 Angle of draw as a function of the opening depth-to-width ratio.....	57
5.7 Maximum subsidence as a function of the opening length-to-width ratio.....	58
5.8 Maximum subsidence as a function of the opening height-to-width ratio.....	59
5.9 Maximum subsidence as a function of the opening depth-to-width ratio.....	60
6.1 Properties of error function curve to represent cross-section settlement trough above tunnel.....	65
6.2 Comparison of the surface settlement trough calculations using values of Z_r and Z_c for $B_s/W = 0.10$, $H/W = 0.5$ and $L/W = 2$	67

LIST OF FIGURES (Continued)

Figure	Page
6.3	Example of comparison of the model simulation subsidence trough and the troughs calculated by different empirical formulae, where $B_s/W = 0.10$, $Z_r/W = 2$, $H/W = 0.5$ and $L/W = 2$
	67
6.4	Surface settlement troughs for different values of Z_r/W where $B_s/W = 0.10$, $H/W = 1$ and $L/W = 5$
	68
6.5	Volumetric ratios as a function of opening height ratio, opening length ratio and opening depth ratio.....
	71
7.1	Surface subsidence before the opening simulation with predefined overburden thickness.....
	74
7.2	Example of PFC ^{2D} model for surface subsidence after the opening simulation.....
	74
7.3	Surface subsidence under various opening depth-to-width (Z/W) ratios.....
	76
7.4	Characteristics of each particle size under the same underground opening geometry.....
	78
7.5	Failure characteristic on first step of the overburden after the opening simulation.....
	79
7.6	Comparisons of the angle of draw (γ) obtained from PFC ^{2D} and physical model test.....
	80
7.7	Comparisons of the S_{max}/W obtained from PFC ^{2D} and physical model test.....
	81

SYMBOLS AND ABBREVIATIONS

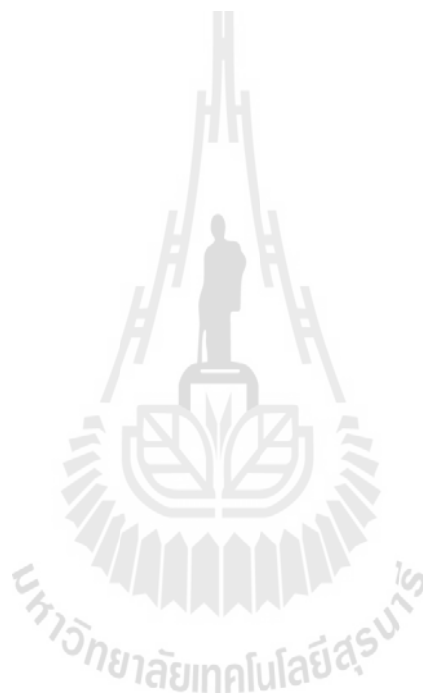
S_{\max}	=	Maximum magnitude of subsidence
γ	=	Angle of draw
$S(x)$	=	Vertical displacement
$G(x)$	=	Slope (or tilt)
$\rho(x)$	=	Vertical curvature
$u(x)$	=	Horizontal displacement (lateral movement)
$\varepsilon(x)$	=	Horizontal strain
b	=	Arbitrary constant
c	=	Arbitrary constant
x	=	Horizontal distance
B	=	Radius of critical area of excavation
Y_{ss}	=	Model parameters represents the steady-state closure rate
Y_o	=	Model parameters represents the ultimate transient closure
β	=	Empirical constants used to model the transient closure rate
N	=	Empirical constants used to model the transient closure rate
t	=	Time since excavation
E	=	Extraction ratio of the mine
Z_u	=	Ultimate surface displacement at any location
C_u	=	Uniformity coefficient
C_c	=	Coefficient of curvature

SYMBOLS AND ABBREVIATIONS (Continued)

D_{10}	=	Particle size at 10% finer
D_{30}	=	Particle size at 30% finer
D_{60}	=	Particle size at 60% finer
τ	=	Shear strength
σ_n	=	Normal stress
c	=	Cohesion
ϕ	=	Friction angle
K_s	=	Joint shear stiffness
K_n	=	Joint normal stiffness
δ_s	=	Shear displacement
δ_n	=	Normal displacement
W	=	Underground opening width
L	=	Underground opening length
H	=	Underground opening height
Z	=	Underground opening depth (or overburden thickness)
B_s	=	Block size (or particle size)
i	=	Width of settlement trough, defined as distance from center to point of inflection of curve
Z_c	=	Distance measured from surface to mid-height of opening
Z_r	=	Distance measured from surface to opening roof
ΔV	=	Change of surface settlement volume

SYMBOLS AND ABBREVIATIONS (Continued)

V_s	=	Volume of surface settlement
V_L	=	Volume of lost ground
V_o	=	Volume of underground opening



CHAPTER I

INTRODUCTION

1.1 Background and rationale

Surface subsidence as a consequence of underground mining and tunneling can impact the environment and surface structures within the mine area (Asadi et al., 2005). Sometimes this subsidence is of little importance to green field sites (i.e., those without surface structures), but it may cause significant damage where surface structures are present. However, even without structures, subsidence can do damage. Many scholars have studied the mechanisms of land subsidence caused by groundwater withdrawal (Murayama, 1961; Lofgren, 1968; Helm, 1975, 1976; Poland, 1977; Holzer, 1981, 1984; Shen et al., 2006). It is widely accepted that the compression of soft clay layers and the compaction of sand is a main cause of land subsidence and time delay of deformation. In order to minimize the environmental impact, a reliable subsidence prediction is essential. One key parameter for subsidence analysis and prediction is the angle of draw, which defines the limits of the area affected by subsidence. Determination of the extent of surface subsidence due to underground mining is important for deciding whether a particular structure is located within the subsiding area or not. It is known that, for particular extraction geometry, the area affected by subsidence is controlled predominantly by geologic conditions in the overburden and by the mining geometry, i.e. lateral extent, thickness, depth, and dip of the seam mined.

Even though extensive study has been carried out in an attempt to understand and predict the surface subsidence behavior induced by underground excavations, the effects of opening geometry under super-critical condition have rarely been addressed. The difficulty in predicting the subsidence under super-critical condition is due to the complexity of the post-failure behavior of the overburden.

1.2 Research objectives

The objective of this study is to develop a trap door apparatus for use in three-dimensional simulations of surface subsidence under various underground opening configurations. The investigation is focused on the angle of draw, maximum subsidence and volume of trough as a function of the opening geometry. The results are obtained from the overburden simulated by using granular materials (cohesionless materials). The simulations are under super-critical conditions, i.e. in plan view the excavation dimensions are sufficient to induce maximum possible subsidence. The test results are compared with subsidence profile predictions obtained from empirical methods for tunnels in fractured rock mass and from discrete element analyses (PFC^{2D}).

The findings can be useful to evaluate the subsidence magnitude and profile for underground mining in fractured rock mass.

1.3 Scope and limitations

1. Scaled-down physical model is constructed in the laboratory with the size of 95×95×60 cm.
2. Subsidence of the model is induced by real gravitational force.

3. Granular materials are selected to simulate the overburden.
4. All tests are made under ambient temperature.
5. Each opening configuration is simulated at least 3 times to verify the repeatability of the results.
6. The opening width is simulated from 50 mm to 250 mm with an increment of 50 mm. The opening length is simulated from 50 mm up to 500 mm with 50 mm increment. The opening height is selected from 10, 20, 30, 40, to 50 mm. The overburden thickness is varied from 50 to 200 mm (at 25 mm intervals).
7. The observed results are compared with numerical analysis (using PFC^{2D} software) and with the empirical calculation of Peck (1969).
8. The main focus is on the super-critical subsidence induced by manmade underground openings (e.g. mines, tunnels and caverns).

1.4 Research methodology

The research methodology shown in Figure 1.1 comprises 6 steps; including 1) literature review, 2) sample collection and preparation, 3) design and fabrication of the test frame, 4) analysis and comparisons the model simulation with computer simulation and empirical calculation, 5) discussions and conclusions and 6) thesis writing and presentation.

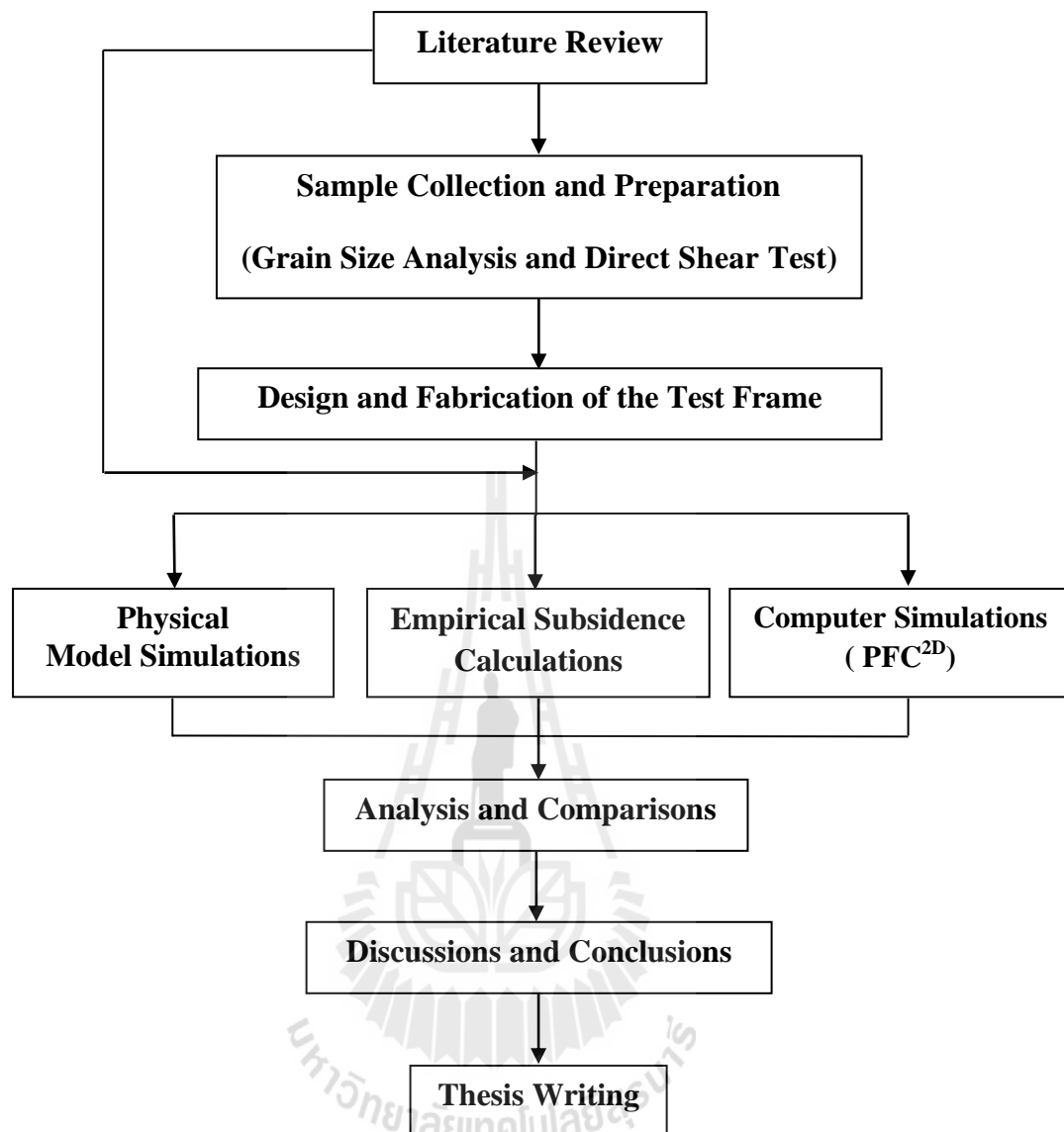


Figure 1.1 Research methodology.

1.4.1 Literature review

Literature review is carried out to improve an understanding of surface subsidence knowledge and case studies in Thailand and abroad. The sources of information are from text books, journals, technical reports and conference papers. A summary of the literature review is given in chapter two.

1.4.2 Sample collection and preparation

Granular materials are primarily selected for model testing. Sample preparations are carried out in the laboratory at the Suranaree University of Technology. Before model testing all materials are subjected to two tests; grain size analysis and direct shear test. The grain size analysis is performed to determine the percentage of different grain sizes contained within a material. The objective of direct shear test is to determine the cohesion and the friction angle of the material.

1.4.3 Design and fabrication of the test frame

A test frame for physical model simulation is designed and constructed in Geomechanic research unit at Suranaree University of Technology. Solid Work program is used to design the test frame. The testing space (area) is about 95×95×60 cm. The physical model is allowed to vary widths, lengths, heights and depths of the underground openings.

1.4.4 Physical model simulation

The physical model is used to simulate subsidence of overburden in three-dimension. The varied parameters are widths, lengths, heights and depths of underground openings and the mechanical properties (ϕ and c) of the overburden. The laboratory testing is measured the maximum magnitude of subsidence (S_{\max}) and the

angle of draw (γ), and hence allowing to study the effect of opening geometries and mechanical properties of overburden.

1.4.5 Empirical Subsidence Calculations

The empirical method given by Peck (1969) is used to predict the subsidence trough profile. Various expressions have been proposed for calculating the trough width at inflection point. Results obtained from this empirical method are compared with the physical simulation results.

1.4.6 Computer simulation

The computer program is used to calculate the characteristics of the subsidence model by considering the effects of underground opening geometries. Calculation is used Particle Flow Code in 2 Dimensions (PFC^{2D}). Discrete element modeling is employed for this study due to its advantages in analyzing large deformations and discontinuous processes.

1.4.7 Analysis and comparisons

Results obtained from model simulations are compared with the computer simulation results and with the empirical solution given by Peck (1969).

1.4.8 Discussions and conclusion

Discussions are made on the reliability and adequacies of the approaches used here. Future research needs are identified. All research activities, methods, and results are documented and compiled in the thesis. The research or findings are published in the conference proceedings or journals.

1.4.9 Thesis writing

All study activities, methods, and results are documented and compiled in the thesis.

1.5 Thesis contents

This research thesis is divided into nine chapters. The first chapter includes background and rationale, research objectives, scope and limitations and research methodology. The second chapter presents results of the literature review to improve an understanding of surface subsidence knowledge and case studies in Thailand and abroad. The Chapter three describes sample preparation. Design and fabrication of the test frame described in chapter four. Physical model simulation in laboratory using a trap door apparatus is explicated in chapter five. Chapter six presents the empirical subsidence calculation for use to predict the subsidence profile in each case. Chapter seven proposes subsidence prediction using discrete element analyses by PFC^{2D}. Comparison and analysis between the results obtained from physical model, empirical method and computer simulation describes in chapter eight. Chapter nine presents discussions, conclusions and recommendation for future studies.

CHAPTER II

LITERATURE REVIEW

2.1 Introduction

Relevant topics and previous research results are reviewed to improve an understanding of surface subsidence and case studies. These include the effects of underground opening geometries on surface subsidence, surface subsidence prediction, physical modeling, empirical subsidence calculation and computer modeling. Initial review results are summarized below.

2.2 Calculation, prediction and monitoring of surface subsidence

2.2.1 Calculation with profile function method

Singh (1992) states that subsidence is an inevitable consequence of underground mining – it may be small and localized or extend over large areas, it may be immediate or delayed for many years. During recent years, with the expansion of urbanization and increased concern for the environment, it is no longer possible to ignore its aftermath.

The major objectives of subsidence engineering are

- 1) Prediction of ground movement.
- 2) Determining the effects of such movements on structures and renewable resource.
- 3) Minimizing damage due to subsidence.

Whenever a cavity is created underground, due to the mining of minerals or for any other reason, the stress field in the surrounding strata is disturbed. These stress changes produce deformations and displacements of the strata, the extent of which depends on the magnitude of the stresses and the cavity dimensions. With time, supporting structures deteriorate and the cavity enlarges, resulting in instability. This induces the superjacent strata to move into the void. Gradually, these movements work up to the surface, manifesting themselves as a depression. This is commonly referred to as subsidence. Thus mine subsidence may be defined as ground movements that occur due to the collapse of overlying strata into mine voids. Surface subsidence generally entails both vertical and lateral movements.

Surface subsidence manifests itself in three major ways:

- 1) Cracks, fissures, or step fractures.
- 2) Pits or sinkholes.
- 3) Troughs or sags.

Surface fractures may be in the form of open cracks, stepped slips, or cave - in pits and reflect tension or shear stresses in the ground surface.

Based on cover depth and panel extraction width, a longwall panel may be classified as being of sub-critical, critical or super-critical width (Figure 2.1). Panel critical width is defined as the panel width for which maximum possible subsidence for a given extraction height is developed. The critical width represents the cross-over point from a “wide and/or shallow” longwall panel to a “narrow and/or deep” longwall panel, the width and depth being determined relative to one another. The magnitude of the critical width depends upon the geological characteristics of the overburden and can range from 1.4 to 2 times the mining depth.

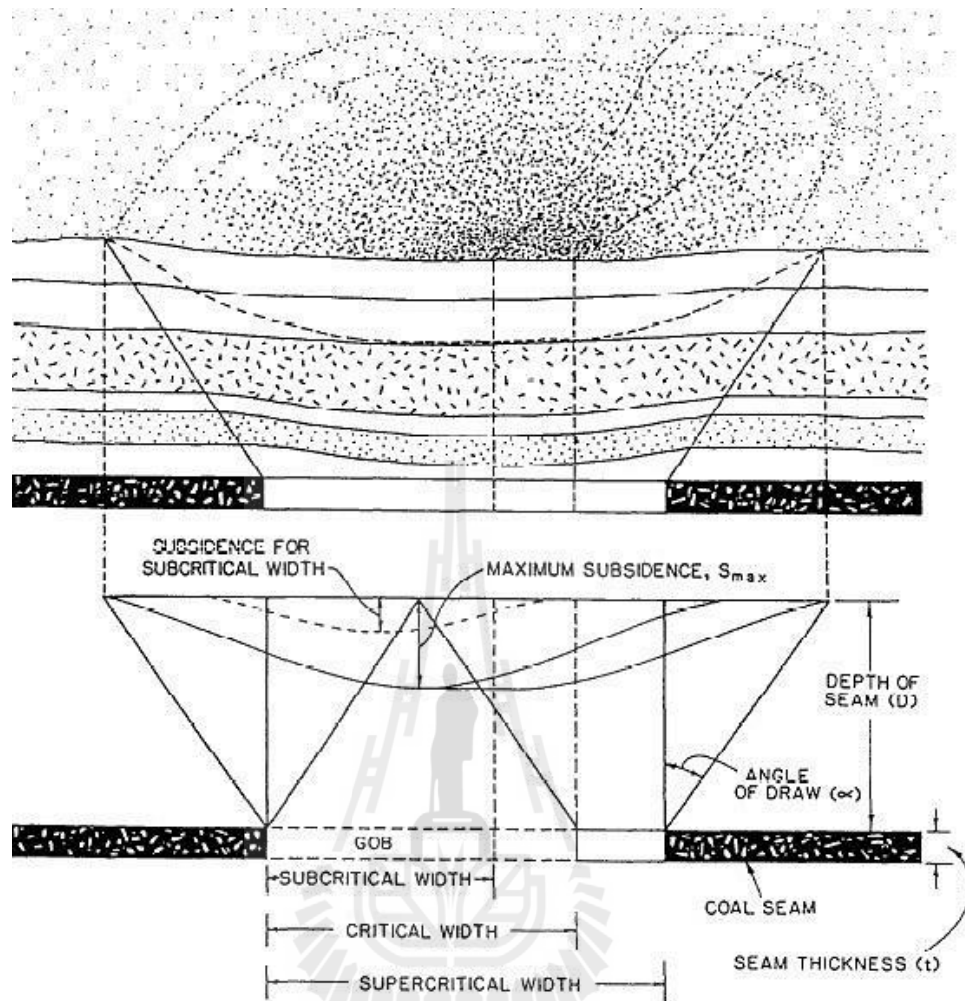


Figure 2.1 Influence of extraction width on subsidence.

Subsidence consists of five major components, which influence damage to surface structures and renewable resources are vertical displacement, horizontal displacement, slope, vertical strain, and vertical curvature (Figure 2.2).

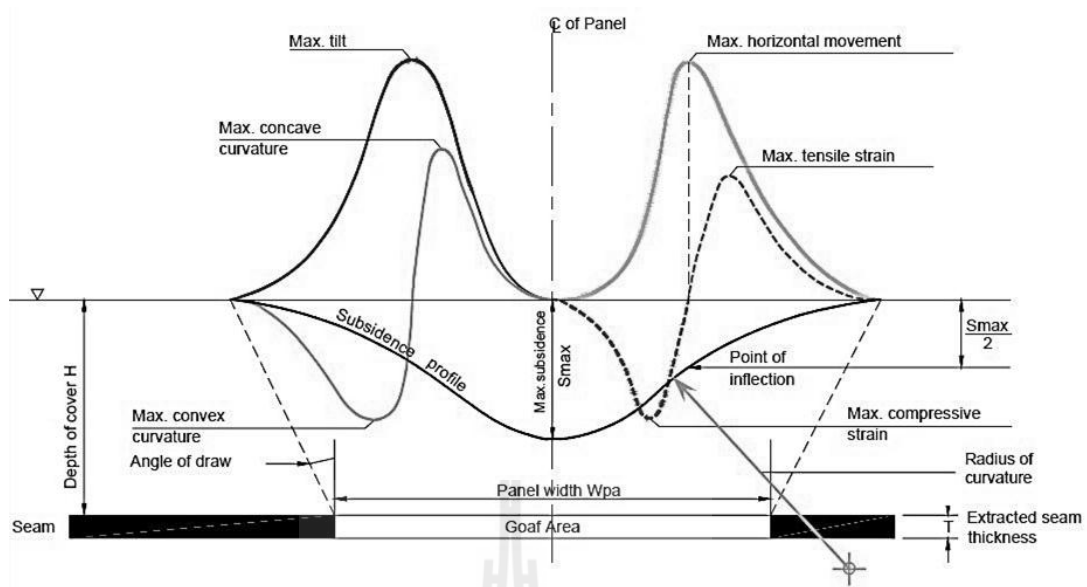


Figure 2.2 Schematic of ground movements caused by subsidence.

Calculation by profile function;

Vertical displacement:

$$S(x) = \frac{1}{2} S_{\max} [1 - \tanh (cx/B)] \quad (2.1)$$

Slope (or tilt):

$$G(x) = S'(x) = -\frac{1}{2} S_{\max} (c/B) \operatorname{sech}^2 (cx/B) \quad (2.2)$$

Vertical curvature:

$$\rho(x) = S''(x) = S_{\max} (c^2/B^2) [\operatorname{sech}^2 (cx/B) \tanh (cx/B)] \quad (2.3)$$

Horizontal displacement (lateral movement):

$$u(x) = -\frac{1}{2} S_{\max} (bc/B) \operatorname{sech}^2 (cx/B) \quad (2.4)$$

Horizontal strain:

$$\varepsilon(x) = S_{\max} (bc^2/B^2) [\operatorname{sech}^2 (cx/B) \tanh (cx/B)] \quad (2.5)$$

where S_{\max} is the maximum subsidence,

D is depth of cavern,

γ is angle of draw,

x is horizontal distance,

c is arbitrary constant, where $c = 1.8$ for critical and supercritical widths, and $c = 1.4$ for subcritical widths

b is constant, and

B is maximum radius of cavern area.

2.2.2 Calculation with SALT_SUBSID program

SALT_SUBSID code developed by RE/SPEC Inc. (Nieland, 1991) has been used to predict the three-dimensional surface subsidence for predicting configurations of solution cavern on top of salt bed. SALT_SUBSID is designed to calculate the subsidence profile induced by dry mining (underground openings) and solution mining (brine caverns). The key parameters used in SALT_SUBSID including Y_{ss} , Y_o , β and N have been calibrated using the subsidence results computed by the finite element analysis. This makes the predicted subsidence profile over the cavern field more site-specific. Definition of these parameters is described in details by Nieland (1991).

$$Z(x,y,t) = Z_u(x,y).G(t) \quad (2.6)$$

$$G(t) = Y_{ss}.t + Y_o[1 - \exp(-\beta E^N t)], \text{ and} \quad (2.7)$$

$$G(t) = 1; \text{ if } Y_{ss}.t + Y_o[1 - \exp(-\beta E^N t)] > 1 \quad (2.8)$$

where Y_{ss} , Y_o , β , N are model parameters,

t is time since excavation,

E is extraction ratio of the mine, and

Z_u is ultimate surface displacement at any location

The condition that $G(t) = 1$ is applied when a cavity is completely closed. The parameter Y_{ss} represents the steady-state closure rate and Y_o represents the ultimate transient closure. The parameters β and N are empirical constants used to model the transient closure rate. In the case of dry mining, the parameter Y_{ss} is set to zero.

2.2.3 Prediction with PFC 2D software

PFC^{2D} (Particle Flow Code in 2 Dimensions) developed by Itasca Consulting Group Inc. (2008). PFC^{2D} is a discontinuum code used in analysis, testing, and research in any field where the interaction of many discrete objects exhibiting large-strain and/or fracturing is required. Because PFC^{2D} is not designed to examine a particular type of problem, its range extends to any analysis that examines the dynamic behavior of a particulate system.

In PFC^{2D}, materials may be modeled as either bonded (cemented) or unbonded (granular) assemblies of particles. Though the code uses circular particles by default, particle shape may be defined in a PFC^{2D} model through use of the built-in clump logic.

The efficient contact detection scheme and the explicit solution method ensure that a wide variety of simulations — from rapid flow to brittle fracture of a stiff solid — are modeled accurately and rapidly. All the equations used in PFC^{2D} are documented. The user has access (via the powerful built-in programming language, FISH) to almost all internal variables. The codes are not “black boxes,” but open software that can be used with confidence.

PFC^{2D} uses an explicit solution scheme that gives stable solutions to unstable processes. It can describe non-linear behavior and localization with accuracy that cannot be matched by typical finite element programs. This makes PFC^{2D}, along with its three-dimensional counterpart PFC3D, the only commercially available codes of their kind.

2.2.4 The monitoring and prediction of mining subsidence

Donnelly et al. (2001) have developed the SWIFT (Subsidence With Influence Function Technique) mining subsidence prediction program, was used to predict mining subsidence across four survey traverses. These were initially installed to monitor mining subsidence during the long wall working of a coal seam. The SWIFT program produced subsidence curves that were similar to the observed data in terms of subsidence trough morphology and general characteristics. However, the SWIFT program overestimated the magnitude of mining subsidence in each case by 0.17 ± 0.20 m. This can be explained by the geological differences between the Carboniferous coal measures of Britain, where the SWIFT program was devised, and the Tertiary coal measures in Colombia.

SWIFT calculations are based entirely on mathematical and geometrical principles. Basically, the subsidence characteristics are derived from the

geometry of the extracted volume and its relationship to the surface. Subsidence is influenced by the geology, stratigraphy, structure, and geotechnical properties of the strata, engineering behaviour of the ground and tectonic setting of the coal basins, but these factors are not included in the subsidence calculations. In Colombia, there are a greater number of igneous horizons, such as intrusive sills and extrusive lava flows, in the region between the mined horizon and the ground surface. In comparison, the coal measures in the Britain Isles do not contain igneous sequences in such abundance. The stronger and more competent igneous horizons would effectively span a greater distance before subsiding. It is likely that this causes bed separation during subsidence, resulting in a reduction in the subsidence of the ground surface.

This research has shown that British-based mining subsidence techniques can be used to predict mining subsidence in Colombia. However, the SWIFT program must be calibrated to suit the local geological and geotechnical conditions. Furthermore, if the subsidence predictions are carried out in conjunction with local geological expertise, and are verified by field observations and monitoring, then can then be a reliable and cost-effective method of subsidence prediction.

Tan et al. (2009) introduce the subsidence coefficient which is a key parameter for ground movement and deformation prediction when mining under the building, water, and railway; so how to get exact subsidence coefficient is one of the most important problems in the discipline of mining subsidence. Support vector machine (SVM) is a new algorithm of machine learning based on statistical learning theory. Compared with traditional method, SVM can be established under condition of deficient samples and abnormal observation result can be rejected effectively. Based on comprehensive analysis of effect factors on subsidence coefficient such as

mechanical characteristics of upper rock stratum, thickness of alluvium deposit, ratio value of mining deepness to thickness, mining method and roof control method, etc, data from tens of typical observation stations was used as training samples, by means of electing kernel function, insensitive loss function, proper penalty factor, regression relation model of SVM was designed between subsidence coefficient and affecting factors. Finally, testing and analyzing was done, and research results show that the SVM relation model can calculate subsidence coefficient and reliable precision can be got, which can meet the requirement of engineering. Research findings prove that the method to calculate subsidence coefficient based on SVM method is feasible. Besides, multiple effect factors can be comprehensively considered with this method, thus a new approach of efficient and accurate calculation of subsidence coefficient is provided for future research.

Oh and Lee (2010) study the weights-of-evidence model that one of the Bayesian probability models was applied in evaluating a ground subsidence spatial hazard near abandoned underground coal mines (AUCMs) at Magyori area, Samcheok City in Korea using GIS. Using ground subsidence location and a spatial database containing information such as mining tunnel, borehole, topography, geology, and land use, the weights-of-evidence model was applied to calculate each relevant factor's rating for the Magyori area in Korea. Seven major factors controlling or related to ground subsidence were determined from the probability analysis of the existing ground subsidence area; depth of drift and distance from drift from the mining tunnel map, slope gradient obtained from the topographical map, ground water level and permeability from borehole data, geology and land use. Tests of conditional independence were performed for the selection of factors, allowing 6

combinations of factors to be analyzed. For the analysis of mapping ground subsidence spatial hazard, the contrast values, W^+ and W^- , of each factor's rating were overlaid spatially. The results of the analysis were validated using receiver operating characteristic (ROC) with the previous ground subsidence locations. In the case of all factor used, the area under the ROC curve (AUC) showed 0.9667, which corresponds to an accuracy of 96.67%. In the case of the combinations, the case of distance from drift, depth of ground water and land use used, showed the 90.71% (AUC: 0.9071) accuracy which is the best result produced in this analysis. The results can be used for hazard prevention and land-use planning near AUCM areas.

Li et al. (2010) introduced a new fuzzy probability measures (FPM) method for prediction of surface subsidence due to inclined coal seam mining. Based on the non-symmetric membership function and the definition of the fuzzy probability measure, the mathematical model for the two-dimensional problem is developed and applied to the analysis of ground subsidence due to underground mining of inclined coal seam. The new method (fuzzy probability measure method) has the following advantages: (1) it is simple, and the theoretical prediction results can be obtained by numerical intergral; (2) it is suitable for the study of ground subsidence due to inclined coal seam and flat seam mining in mountainous areas; and (3) results are presented to demonstrate the advantages of the proposed method over traditional stochastic medium theory (SMT) procedures in terms of accuracy and stability. The results of calculation with the new model indicate that the predicted value has good agreement with the measured data.

2.3 Physical modeling

Physical modeling has played an important role in studies related to stability of underground mines and tunnels. A variety of modeling techniques have been developed all over the world to study ground response to underground excavation and tunneling. These techniques range from the two-dimensional trap door tests to the miniature tunnel boring machines that simulate the process of tunnel excavation and lining installation in a centrifuge (Meguid et al., 2008).

Caudron et al. (2006) studied soil-structure interaction during a sinkhole phenomenon using an analog two-dimensional soil and a physical model and a numerical method. They use bidimensional Schneebeli material (Figure 2.3) in a small-scale model allowing fully controlled test conditions. The Schneebeli material is modified in order to exhibit a cohesive frictional behavior. The physical model allows to represent a case of study and to determine it completely with a limited set of parameters.

Terzaghi (1936) used a model, characterized as the trap-door model. He explained the arching theory based on the translation of a trap door into the soil (passive mode) or away from it (active mode) as shown in Figure 2.4. The passive mode can be used to evaluate of the uplift force of anchors and other buried structures that can be idealized as anchors. The active mode can be used to study the silo problem or the earth pressure on a tunnel lining. According to this model, the deforming arch of a tunnel can be investigated by a downward moving trap-door while the soil above the tunnel can be represented by a layer of granular or slightly cohesive soil. Based on this simple model, the evolution of the mean vertical pressure acting on the trap-door during its downward movement can be studied.

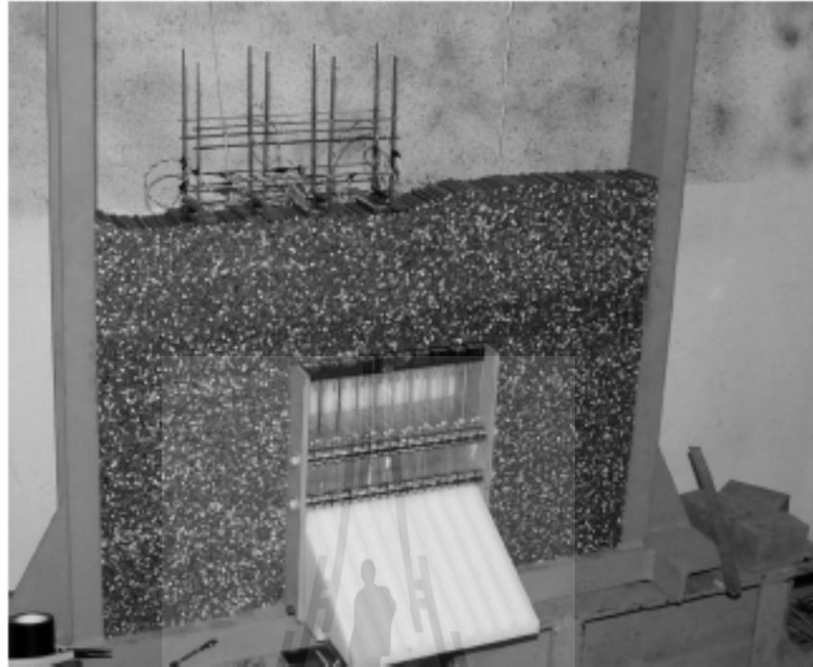


Figure 2.3 Small-scale experimental model (Caudron et al., 2006).

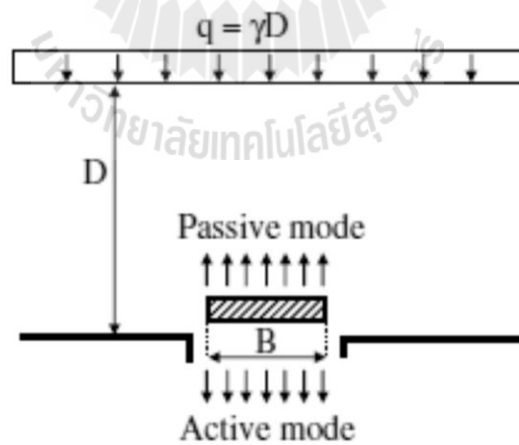


Figure 2.4 Classical trap door problem (Terzaghi, 1936).

The physical model allowed him to represent a case study and to determine it completely with a limited set of parameters.

Park et al. (1999) conducted a series of trap door experiments to investigate the response of inclined layers to tunnel excavations. The tested material consisting of aluminum rods and aluminum blocks was arranged in layers making angles with the horizontal. Figure 2.5 shows an example of the surface settlement profiles induced by lowering the trap door 2 mm for different layer inclination angles and overburden pressures. The inclination angle was found to have a significant effect on the surface settlement trough. Symmetrical settlement profiles were observed for the vertically arranged blocks. For the inclination angles = 30 degrees, the maximum surface settlement shifted towards a direction normal to the layer inclination angle (left of the trap door). Different behavior was found for the case of inclination angles = 60 degrees where the maximum surface settlement shifted in the direction of the layer inclination angle (right of the trap door).

Park et al. (2004) states that surface subsidence causes damage such as the failure and deterioration of buildings, infrastructures, dams, underground utility lines, ground water regimes, etc., resulting in severe economic loss and environmental hazards. The major cause of subsidence is underground mining activities. In order to minimize or prevent subsidence damage, it is necessary to understand subsidence phenomena. It is difficult to simulate or predict subsidence development because of the complexity in physical characteristics such as rock failure and yield behavior, dimensional variations and time dependent behavior. In this paper a new physical subsidence modeling technique is introduced. The method utilizes laser optical

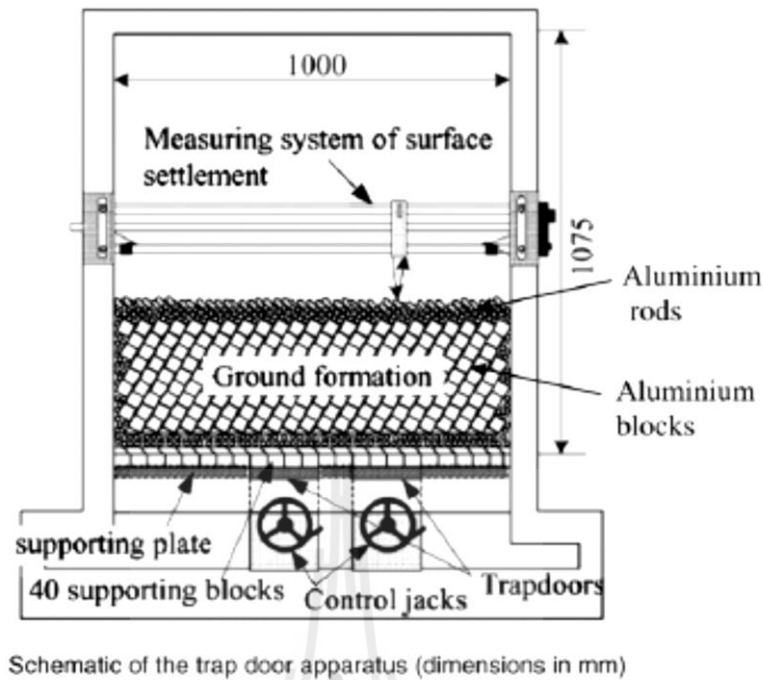


Figure 2.5 Surface settlement profiles induced by the trap door apparatus

(Park et al., 1999).

triangulation distance measurement devices, which can scan the surface of any material, including granular or viscous materials, and digitally measure vertical distances with an extremely high accuracy and resolution. With this new technique, the effect of cavity shape and size, depth, and material parameters can be analyzed. Using this unique technology and method of analysis, significant results were produced. Subsidence profiles, subsidence factors, and angles of draw were analyzed. This research is being continued using the same technique for simulating subsidence with different model materials for various underground cavity dimensions, tunneling, and time dependent subsidence phenomena.

However, the cost of construction and time constraints relative to the immediate needs of an active mine often limit the usefulness of physical modeling.

2.4 Empirical subsidence calculations

Empirically derived relationships are one of the principal methods of predicting mining and tunneling subsidence. This technique is based on the experience gained from a large number of actual field measurements. The empirical methods are quick, simple to use, and yield fairly satisfactory results.

Migliazza et al. (2009) studied the soil subsidence induced by the construction of a shallow underground excavated in a sandy soil by using a mechanized tunnel technique has been undertaken by using empirical, analytical and numerical methods. Also, the purpose of the work was to analyze the performance of the different methods utilized in order to foresee the soil settlements induced in an urban area by the EPB-S machine. The evaluation of the predictable capabilities of the different methods was determined through a comparison of empirical, analytical and numerical results, and the experimental measurements gathered during the examined tunnel construction.

The 3D FEM that considers an elasto-plastic soil behaviour was designed to simulate about 38 m of tunnel construction. The histories of the evolution of the vertical settlements and the subsidence basin were computed, and the numerical results compared with the experimental measurements. The optimum agreement between the numerical and experimental data confirms the 3D elasto- plastic FEM to be a valid tool for evaluating the stress–strain behaviour of the subsoil and for designing interactive support structures.

Fattah et al. (2013) compared the shape of the settlement trough caused by tunneling in cohesive ground by different approaches: analytical, empirical, and numerical. Their study showed that the finite element method overpredicted the

settlement trough width compared with the results from empirical solutions of Peck (1969) for soft and stiff clay, but are in excellent agreement with Rankin's (1988) estimation. An empirical profile or influence function method requires knowledge of maximum possible subsidence (S_{\max}) or maximum subsidence occurring (S), which is related to S_{\max} by a function related to width: depth ratio of extraction (Baghuguna et al., 1991).

2.5 Computer modeling

Numerical methods have a distinct advantage over physical modeling in terms of cost and time. However, extreme care must be taken to insure that the numerical model is an accurate reflection of physical reality.

Mcneary and Barker (1998) compared physical and numerical models of the block-caving mining methods. PFC^{2D} program was used in an attempt to better understand the deformations and flow within each of the physical models during the draw procedure. Bridging and interlocking of the blocks occurred in approximately the same places and similar times during the draw sequence. The results show that the draw down patterns and the rate of draw generated within the numerical models were very similar in development of the physical models. For the given cases of the physical model, the numerical model simulated the behavior of the physical model quite well. The only constraints that were placed on the numerical models were the initial boundary conditions of the physical models. By inspection, the overall shape and flow lines of both the numerical and physical models were extremely close in area removed and flow characteristics. The numerical results as reported in this study are the result of the internal algorithms of the PFC^{2D} program.

Ren and Li (2008) studied the extent of mining subsidence affected area is defined by the limit angles, which is predominantly controlled by geological conditions of the overburden strata and the mining configurations, including seam inclination angle. From observational data worldwide and numerical modeling analysis the following conclusions are drawn: The stiffness, strength and failure of the overburden play an important role in the characteristics of subsidence limit. When overburden rocks are sufficiently strong and no major failure or break up taking place in the roof, the limit angle would tend to be greater in roof rocks with higher stiffness. However, if the roof collapses, stronger strata would produce lower limit angle at the surface and weak roof strata would result in greater limit angle. When there is an adequately strong and stiff rock bed in the overburden, it is possible for a sub-critical subsidence profile to be developed over a panel of super-critical width. The rock strength and stiffness also affect the magnitude of the maximum subsidence. Generally the maximum subsidence over a strong overburden is less than that over a weak overburden. Numerical model has demonstrated that the effect of seam inclination is such that it increases the limit angle at the dip-side of the panel and reduces the limit angle at the rise-side. The values of limit angles over inclined seams may be established from observed data set. Empirical relationship between the limit angles and the seam inclination angle may be derived either using numerical modeling techniques or observed data set in a specific mining field.

Shahriar et al. (2009) studied the surface subsidence due to inclined very shallow coal seam mining of two underground coal mines in Parvadeh (Tabas) coalfield was simulated by FLAC^{3D} code which is based on finite difference method (FDM). FDM results were compared with measured profile and profile function

method. FDM underestimated S_{\max} up to three per cent in comparison with surveying and profile function. The reason is that the residual subsidence is neglected in this research but the profile function method predicts final subsidence trough. Furthermore in both cases, FDM in contrast with measured profiles obtained by surveying and profile function method, predicted uplift over the panels rise side at the surface in which was confirmed by local observations. The reason that no uplift was observed in measured profile provided by Asadi et al (2005) was due to their efforts just have been focused on measuring downwards subsidence. The Position of S_{\max} in shallow coal seams shifted towards panel rise side which was totally in contrast with deep seam mining. Sensitivity analysis showed that by increasing the depth, this point gradually shifts toward the panel dip side. It was also found that critical width to depth ratio range is between 1.0 and 1.4 for both panels. This range is a little lower than the range of critical W/H ratio. This might be related to very low depth situation of both panels. Numerical methods can illustrate subsidence mechanism better than profile function due to taking into account the geomechanical material properties. Accordingly profile function results can hardly be extrapolated from one coal mining area to another, and even sometimes from panel to panel. Empirical methods have their own advantageous because of their simple and inexpensive applications.

Li and Wang (2011) used Particle Flow Code (PFC) to simulate the process of subsidence and to calculate the distribution of contact force and displacement of ore particles, which have a good consistency in comparison with the actual survey data in Shandong province. PFC^{2D} well simulates the process of the mine collapse. Particle flow method has unique advantages in the simulation of mechanical behavior of broken ore particles, in the mechanical analysis of collapse process and in the collapse

displacement of ores. Discrete element modeling is employed for this study due to its advantages in analyzing large deformations and discontinuous processes.

Guo et al. (2011) used numerical models to simulate the surface subsidence of the strip pillar mining. Numerical simulation models were set up to simulate the surface subsidence in different mining depths. The simulated results were compared and analyzed. They found that the surface subsidence law of strip pillar mining is similar to that of full extraction, but the surface subsidence mechanism of strip pillar mining is different from that of full extraction. The result demonstrated that the subsidence of strip pillar mining increases with the increase of mining depth by logarithmic relationship. This is because the weight of the overburden strata increases. Then the loads acted on strip coal pillars and gob material become larger. The strip coal pillars are more compressed and gob materials are also densely compressed. Therefore, both the surface subsidence value and the subsidence factor become larger.

2.6 Effect of underground opening geometries and overburden properties on surface subsidence

Jiang and Yin (2014) investigated the influence of soil conditions on the ground deformation during longitudinal tunneling using discrete element modeling. Different cases of soil conditioning were modeled by reducing the inter-particle friction of soils in the specified zone around the cutter head of the tunnel. The results show that the distance between the biggest surface settlement and the final cutter face is decreasing with the increase of inter-particle friction and the surface settlement increase with increasing fluidity in the conditioning zone.

Dai et al. (2011) studied the relationship between the unconsolidated layers thickness and surface movement by employed FLAC^{3D}. They found that the surface subsidence extends widely and the surface deformations are decreased with the increase of the unconsolidated layer thickness (Figure 2.6). This study is significant to predict surface subsidence of thick unconsolidated layers for coal mine and take effective measures to control surface subsidence.

Papamichos et al. (2001) investigated the consequences of the large reservoir compaction on the surface subsidence of the overburden formations using circular retracting trap door (Figure 2.7) under various overburden heights. Tests with various overburden heights showed the formation of shear bands starting almost vertically at the trap door edges and converging successively to the symmetry axis. In the shallow mechanism, the shear bands reach immediately the upper surface and thus the trap door displacement is felt immediately at the surface as subsidence. In the deep mechanism, at low trap door displacements the shear bands meet initially each other forming an arch and thus only part of the trap door displacement is felt at the surface. The surface subsidence bowl is concentrated primarily above the trap door area.

Yao et al. (1991) introduced an analytical calculation model for the angle of draw by the use of a finite element model proposed by Reddish (1989) at the Nottingham University. They studied the influence of overburden strength and different rock mass properties, and the presence of a distinct bed, on subsidence limit characteristics. Their results show that the angle of draw is related to the overburden properties, depth and configurations of the mine openings.

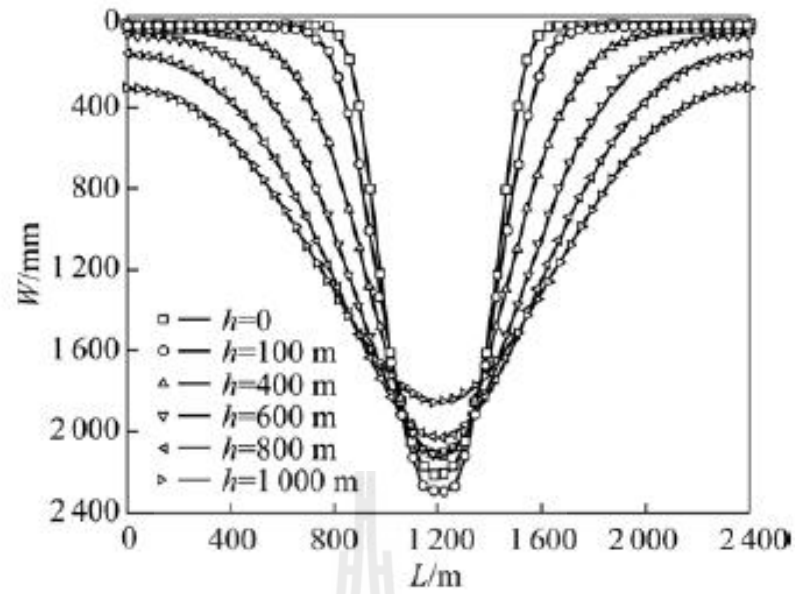


Figure 2.6 Surface subsidence curves of different unconsolidated layers thickness (Dai et al., 2011).

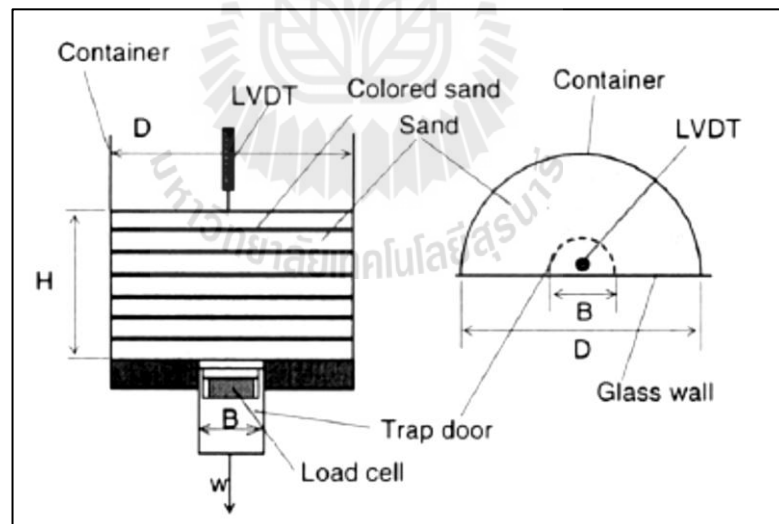


Figure 2.7 Schematic of the trap door apparatus (Papamichos et al., 2001).

Five cases have been studied in order to investigate the effect of different rock mass properties on the angle of draw. The relationship between the percentage of maximum subsidence and the relevant angle of draw for each case has been examined. The results show that increasing the strength of the cover rock mass reduces the angle of draw.

For the effect of strong and weak beds in the overburden on the angle of draw, it can be seen that the weak bed in the overburden increases the angle of draw. Additionally, it is also important to note that a decrease in the uniaxial compressive strength in the weak bed causes a significant increase in the angle of draw. However, it seems that with an increase in the uniaxial compressive strength of the strong bed, the angle of draw decreases only slightly.

Ren and Li (2008) studied the mechanism of stratum movements and the associated subsidence limit at ground surface. The results indicate that the extent of surface subsidence is defined by the limit angles, which is controlled by geological conditions of the overburden strata and the mining configurations. When overburden rocks are sufficiently strong and no major failure or break up taking place in the roof, the limit angle would tend to be greater in roof rocks with higher stiffness. However, if the roof collapses, stronger strata would produce lower limit angle at the surface and weak roof strata would result in greater limit angle. The rock strength and stiffness also affect the magnitude of the maximum subsidence. The maximum subsidence over a strong overburden is less than that over a weak overburden.

Thongprapha et al. (2015) used physical model simulations to determine the effects of underground opening configurations on surface subsidence under super-critical conditions. A trap door apparatus has been fabricated to perform the scaled-

down simulations of surface subsidence. Clean gravel is used to represent the overburden in order to exhibit a cohesionless behavior. The effects of opening length (L) and opening height (H) are assessed by simulating the L/W from 1, 2, 3, 4 to 5 and H/W from 0.2, 0.4, 0.6, 0.8 to 1, where W = 50 mm. The effect of opening depth (Z) is investigated here by varying Z/W from 1 to 3 to 4. The results indicate the angle of draw the maximum subsidence and the volume of trough are controlled by the width, length, height and depth of the underground openings. The angle of draw and maximum subsidence increase with increasing L/W ratio and tends to approach a limit when L/W equals 3. For the same L/W ratio and H/W ratio, increasing the Z/W ratio reduces the angle of draw and maximum subsidence. The volume of subsidence trough observed from the physical model is always less than the opening volume. This is due to settlement in the physical model has created new voids above the opening. However, the subsidence trough volume tends to decrease as the opening depth increases, particularly for short opening.

2.7 Previous relevant researches

Asadi et al. (2005) proposed a new profile function. It is formed from the sum of two negative exponential functions that have been adjusted to three survey lines in a case study in the Negin coalmine east of Iran. Because of the simplicity of the profile function, the use of the new model decreases the calculation time for predicting surface subsidence and enhances the precision of subsidence prediction. The results gained from surface subsidence measurements at Negin coalmine show an excellent correlation between the measured and the predicted subsidence by using the new model. The correlation coefficient was 0.999, which is very high.

In the empirical method, different graphs and tables are given for different conditions and geometrical shapes. It is possible to predict the amount of subsidence using these graphs and tables. The National Coal Board (NCB) has suggested one of the most well-known graphs for the prediction of subsidence. For example, a graph for the prediction of surface subsidence in horizontal stopes is given in Figure 2.8.

In the physical method, by combining different materials such as sand and gelatin, a real model, but smaller than the extracted area, has been built. By precise monitoring and processing of data, the amount of subsidence in a real condition is calculated. An example of the physical model is given in Figure 2.9. In numerical methods, displacements and subsidence of ground surface can be calculated by using finite elements, boundary elements, distinct elements, and finite difference methods. Application of a computer for solving very complex equations in diverse initial and boundary conditions with different material behaviour made numerical methods more popular in the prediction of subsidence. In this regard, different software has been developed to consider inhomogeneous and anisotropic behaviour of rock mass worldwide.

Aracheeploha et al. (2009) developed an analytical method to predict the location, depth and size of caverns created at the interface between salt and overlying formations. A governing hyperbolic equation is used in a statistical analysis of the ground survey data to determine the cavern location, maximum subsidence, maximum surface slope and surface curvature under the sub-critical and critical conditions. A computer program is developed to perform the regression and produce a set of subsidence components and a representative profile of the surface subsidence under sub-critical and critical conditions. Finite difference analyses using FLAC code correlate the subsidence components with the cavern size and depth under a variety of

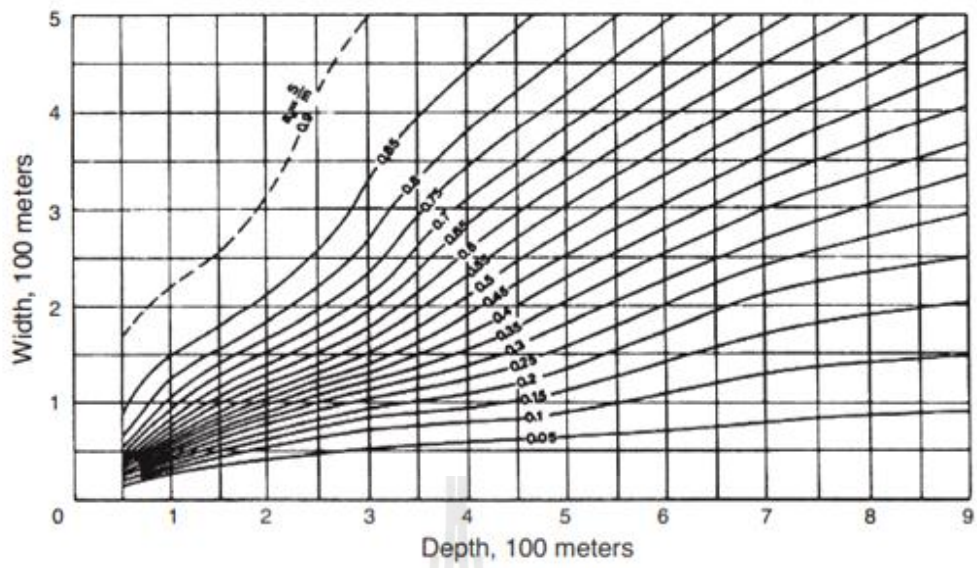


Figure 2.8 Graph suggested by NCB (Asadi et al., 2005).

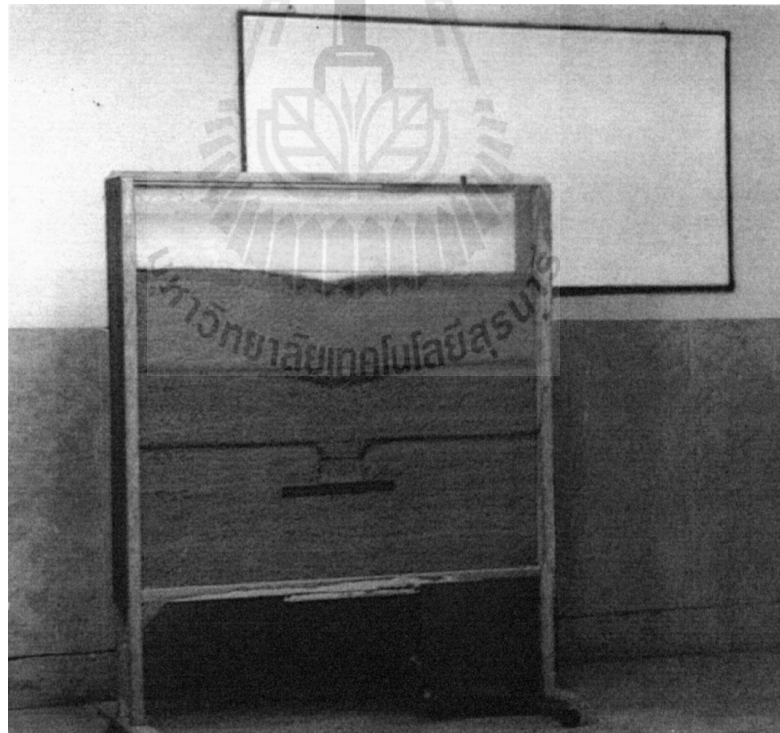


Figure 2.9 Physical model for prediction of subsidence (Asadi et al., 2005).

strengths and deformation moduli of the overburden. Set of empirical equations correlates these subsidence components with the cavern configurations and overburden properties. For the super-critical condition a discrete element method (using UDEC code) is used to demonstrate the uncertainties of the ground movement and sinkhole development resulting from the complexity of the post-failure deformation and joint movements in the overburden. The correlations of the subsidence components with the overburden mechanical properties and cavern geometry are applicable to the range of site conditions specifically imposed here (e.g., half oval-shaped cavern created at the overburden-salt interface, horizontal rock units, flat ground surface, and saturated condition). These relations may not be applicable to subsidence induced under different rock characteristics or different configurations of the caverns. The proposed method is not applicable under super-critical conditions where post-failure behavior of the overburden rock mass is not only unpredictable but also complicated by the system of joints, as demonstrated by the results of the discrete element analyses. The proposed method is useful as a predictive tool to identify the configurations of a solution cavern and the corresponding subsidence components induced by the brine pumping practices as shown in Figure 2.10.

Even though extensive study has been carried out in an attempt to understand and predict the surface subsidence behavior induced by underground excavations, the effects of opening geometry under super-critical condition have rarely been addressed. The difficulty in predicting the subsidence under super-critical condition is due to the complexity of the post-failure behavior of the overburden.

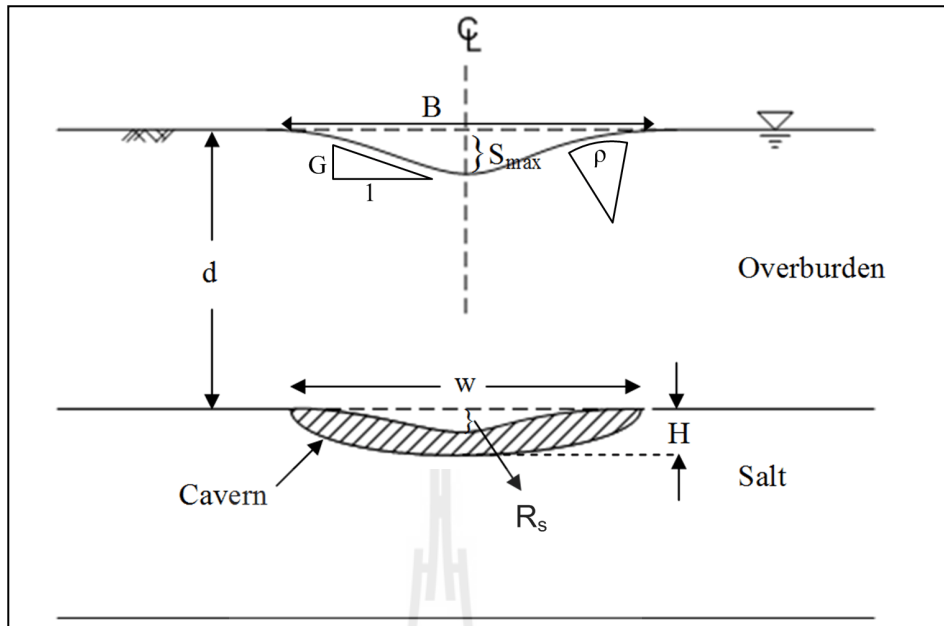


Figure 2.10 Variables used by Aracheeploha et al. (2009).

CHAPTER III

MATERIAL CHARACTERISTICS

3.1 Introduction

This chapter describes the material used to simulate overburden in the physical model simulations. The types of material used in this study are granular materials (cohesionless soil). The granular materials are used to simulate the settlement of overburden under super-critical condition. The materials are subjected to grain size analysis and direct shear testing. Their mechanical properties are used as parameters in the computer simulations.

3.2 Sample preparation

Three size ranges of clean granular materials are used to simulate the overburden in the physical model.

3.2.1 Grain size analysis

The grain size analysis is performed to determine the percentage of various particle sizes and to classify the material (Figure 3.1). The test method and calculation follow the ASTM (D422-63) standard practice. The materials are as follows:

Sample 1 has particle diameters from 0.425 to 2.36 mm, with more than 65.20% of 2 mm diameter (Figure 3.2(a)).

Sample 2 has particle diameters from 2.00 to 6.35 mm, with more than 72.32% of 4.75 mm diameter (Figure 3.2(b)).

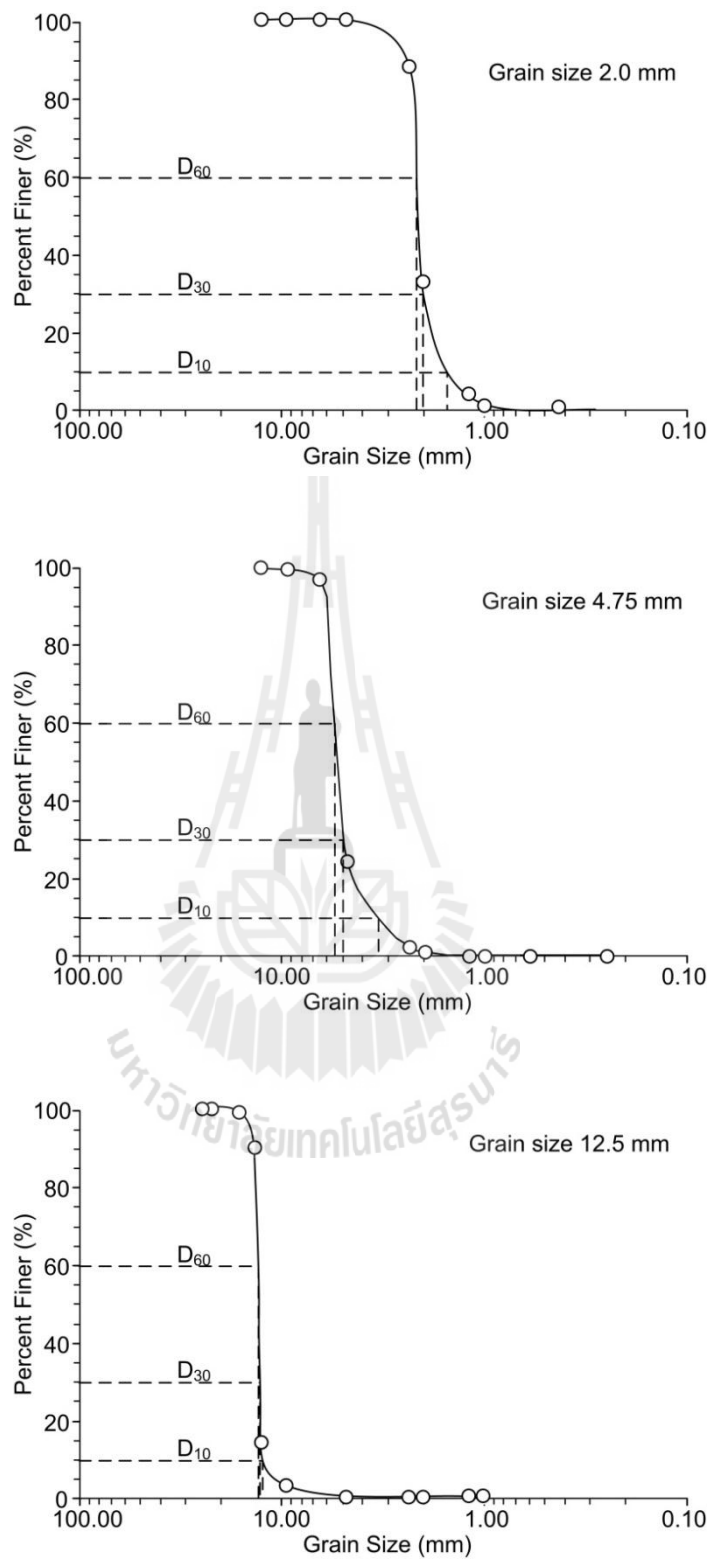


Figure 3.1 Grain size distribution curves of tested materials.

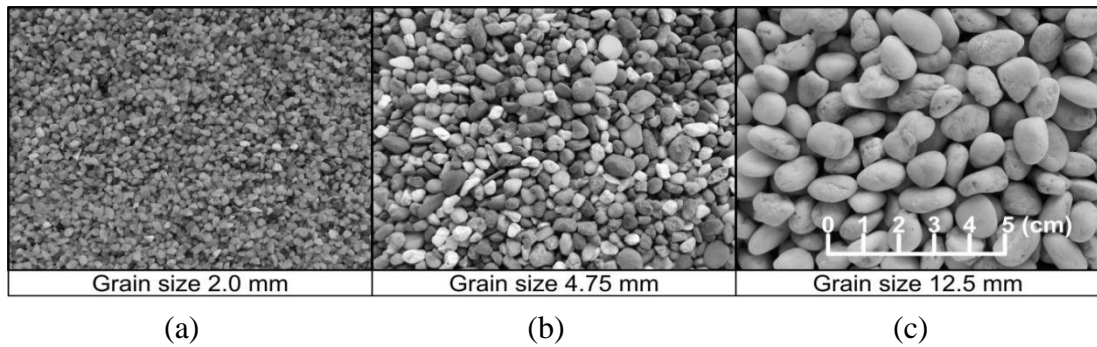


Figure 3.2 Granular materials used to simulate overburden.

Sample 3 has particle diameters from 9.50 to 13.50 mm, with more than 75.43% of 12.5 mm diameter (Figure 3.2(c)).

The unit weights of the materials are 1455, 1530 and 1567 kg/m³, respectively. To classify the gravel in accordance with ASTM (D2487–06) the uniformity coefficient (C_u) and the coefficient of curvature (C_c) are determined as follows:

$$C_u = D_{60}/D_{10} \quad (3.1)$$

$$C_c = D_{30}^2 / (D_{10} \times D_{60}) \quad (3.2)$$

where D_{60} is particle size at 60% finer, D_{30} is particle size at 30% finer and D_{10} is particle size at 10% finer. The uniformity coefficient and the coefficient of curvature for all materials are shown in Table 3.1.

The following classification criteria are in accordance with the Unified Soil Classification System:

For a well graded, the following criteria must be met:

$$C_u > 4 \ \& \ 1 < C_c < 3$$

Table 3.1 Grain size analysis.

Samples	Average size (mm)	C_u	C_c	Type of soil	Grain Shape	
					Sphericity	Roundness
1	2.0	1.29	1.07	Poorly-graded sand	High sphericity	Subangular
2	4.75	1.62	1.34	Poorly-graded gravel	Low sphericity	Rounded
3	12.5	1.50	1.19	Poorly-graded gravel	Low sphericity	Well-rounded

If both of these criteria are not met, the gravel is classified as poorly graded or GP. If both of these criteria are met, the gravel is classified as well graded or GW.

For a well graded, the following criteria must be met:

$$C_u \geq 6 \text{ \& } 1 < C_c < 3$$

If both of these criteria are not met, the sand is classified as poorly graded or SP. If both of these criteria are met, the sand is classified as well graded or SW.

The material in this study is classified as poorly graded sand (SP) and poorly graded gravel (GP). Additionally, the gravels are distinguished the grain shape. Estimation of roundness and sphericity of granular particles is compared with the Power (1953) classification system (Figure 3.3), as shown in Table 3.1

3.2.2 Direct shear test

The direct shear test is performed to determine the cohesion and friction angle of the materials. A circular shear box with 190.5 mm diameter and 152.4 mm thick is used. The test method and calculation follow the ASTM (D5607-08) standard practice. The constant normal stresses are 80, 160, 240, and 320 kPa. Each specimen is sheared once under the predefined constant normal stress using a direct shear device (SBEL DR44), as shown in Figure 3.4. The shearing rate is 20 kPa/s. The shear force is

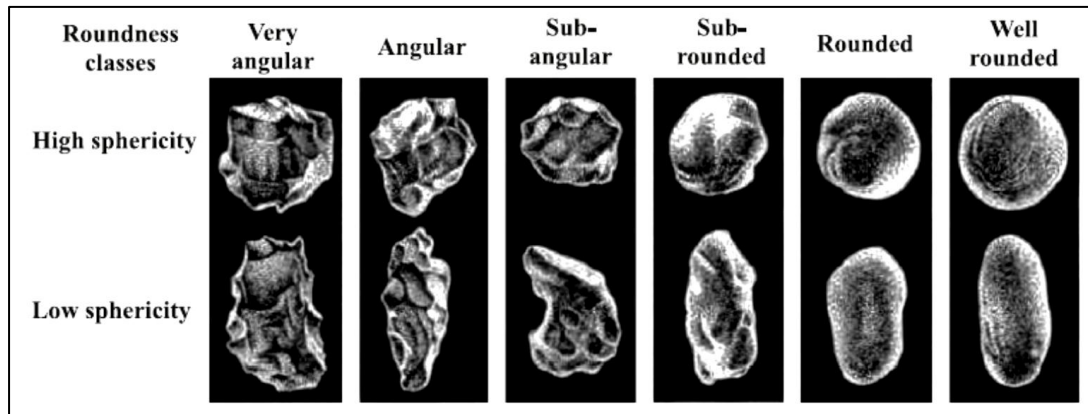


Figure 3.3 Estimation of roundness and sphericity of sedimentary particles (adapted from Powers, 1953).



Figure 3.4 Direct shear device SBEL DR44 used in this study.

continuously applied until a total shear displacement of 8 mm is reached. The applied normal and shear forces and the corresponding normal and shear displacements are monitored and recorded.

Figure 3.5 shows shear stress as a function of shear displacement. The peak and residual shear strengths as a function of the normal stress of each material are shown in Figure 3.6. The shear strength (τ) is calculated based on the Coulomb's criterion (Jaeger et al., 2007: section 4.5) as follows:

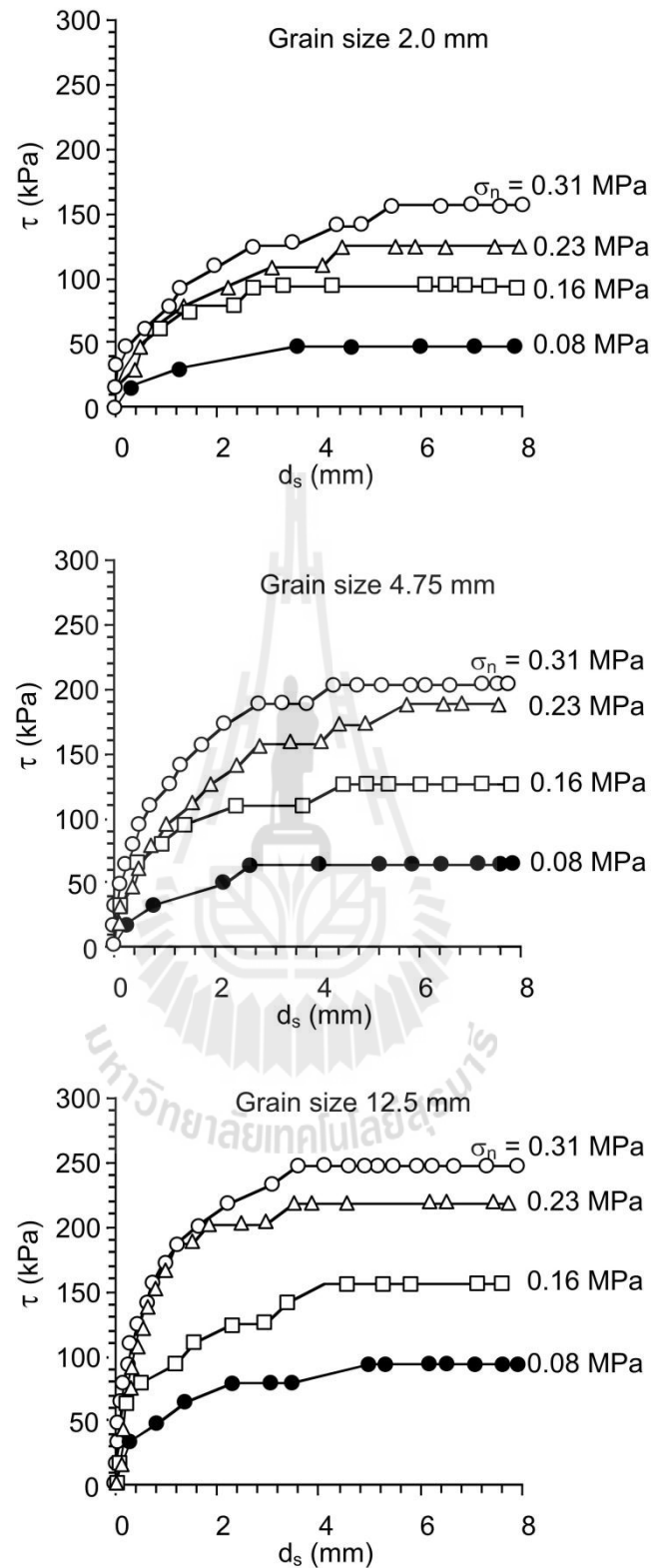


Figure 3.5 Shear stresses as a function of shear displacement.

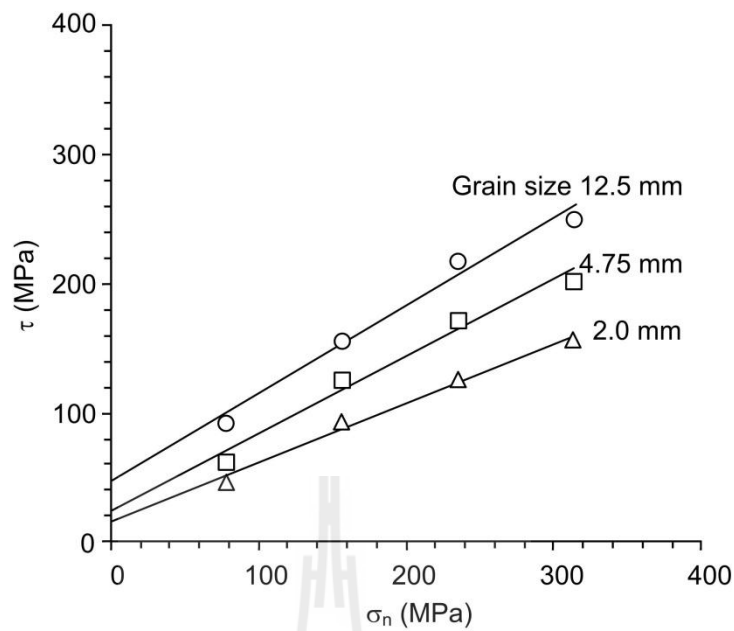


Figure 3.6 Shear strength as a function of normal stress obtained from direct shear testing.

$$\tau_p = c_p + \sigma_n \tan \phi_p \quad \text{for peak shear strength} \quad (3.3)$$

where σ_n is the normal stress, c_p is the peak cohesion and ϕ_p is the peak friction angle. The cohesion for both peak and residual shear strengths the friction angle. The angle of shearing resistance is generally increasing with increasing median particle diameters.

The granular materials are classified as cohesionless soil according to the size of particles with diameter greater than 0.067 mm. Here, the peak friction angle is equal to the residual friction angle. This is because the gravel sample is lightly packed in the shear boxes before shearing primarily to obtain the condition similar to the gravel sample used in the physical model simulation. The loose gravel under low normal load can maintain the same shearing constant from peak through

the residual region. Similar results have been obtained by Raymond (1997) and Kim and Ha (2014) who perform shear tests on cohesionless materials.

The shear stiffness for various normal stresses is calculated at the 50% peak stress using an equation (Jaeger et al., 2007):

$$K_s = \tau_s / \delta_s \quad (3.4)$$

where K_s is the joint shear stiffness (MPa/m), τ_s is the shear stress (MPa), δ_s is the shear displacement (m).

The normal stiffness is calculated by (Jaeger et al., 2007):

$$K_n = \sigma_n / \delta_n \quad (3.5)$$

where K_n is the joint normal stiffness (MPa/m), σ_n is the normal stress (MPa), δ_n is the normal displacement (m). These properties are used in the discrete element analyses (PFC^{2D}). The mechanical properties of granular materials used in this study shown in Table 3.2.

Granular materials are composed of particles of complex shape which are common in nature and also in various fields of science and engineering. These particle shape angularity characteristics strongly affect to the rheology (flow) of particles and to the behavior of sheared granular materials. The existing research results suggest that the internal friction coefficient decrease rapidly with decreasing angularity (Azéma et al, 2012). The more angular particle the greater resistance to the forcing loads and the flowability is reduced (Wang et al., 2011). This is due to a low

Table 3.2 Mechanical properties of tested granular materials.

Samples	Sample sizes (mm)	Bulk density (kN/m ³)	Cohesion (kPa)	Friction angle (ϕ)	Normal stiffness, K_n (MPa/m)	Shear stiffness, K_s (MPa/m)
1	2.0	1455	15.61	24.7	1590.72	26.07
2	4.75	1530	23.42	30.9	901.80	34.39
3	12.5	1567	46.83	34.2	617.86	45.54

angularity particle can rolls and slides more readily than the high angularity particle.

The effect of particle size however is also important here.



CHAPTER IV

TRAP DOOR APPARATUS

4.1 Introduction

A trap door apparatus has been developed for use to simulate subsidence of overburden in three dimensions and to assess the effects of the geometry of underground openings on the surface subsidence. This chapter describes the design requirements and components of the apparatus.

4.2 Design and fabrication of the test apparatus

The functional requirements for the test frame are (1) to simulate subsidence of overburden in three-dimension, (2) to assess the effect of overburden properties and of the geometries of underground openings on the surface subsidence, (3) to observe subsidence of overburden in three-dimension, and (4) to induce subsidence of overburden using real gravitational force.

The physical model (Figure 4.1) comprises three main components: the sample container, the mine opening simulator, and the surface measurement system.

The sample container is filled with materials, in this case, granular materials used to simulate overburden. A custom-made $95 \times 95 \text{ cm}^2$ clear acrylic plate with 15 mm thick is placed in the grooves of the square steel frame. Four acrylic sheets are secured with a steel plate at each side. The testing space is $95 \times 95 \times 60 \text{ cm}^3$.

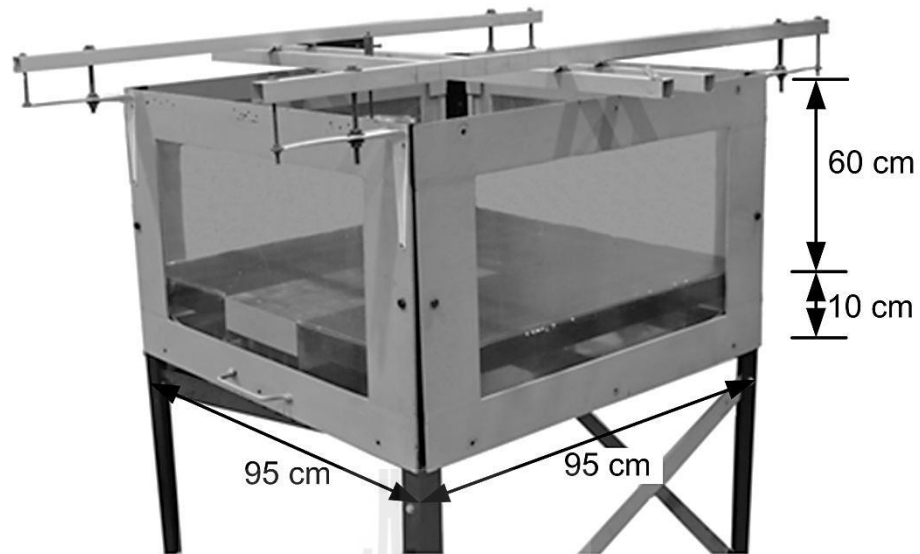


Figure 4.1 Trap door apparatus used in this study.

The mine opening simulator is an array of wooden blocks with sizes of $5 \times 5 \times 10 \text{ cm}^3$. The wooden blocks are arranged in ten columns with five blocks for each column. Fifty small blocks can be gradually and systematically moved down to simulate underground openings with different geometries and hence inducing the subsidence of the overburden. The mine opening simulator is installed underneath the sample container.

The measurement system of the surface subsidence includes a sliding rail with a laser scanner. To measure the surface subsidence under various underground opening geometries, the laser scanner is moved horizontally in two directions. The precision of the measurements is one micron. The results are recorded and plotted as three-dimensional profiles. The maximum subsidence values, angles of draw, slopes and volume of the subsidence trough can be readily determined for each opening configuration. Figures 4.2 through 4.6 illustrate the schematic drawings of the test apparatus.

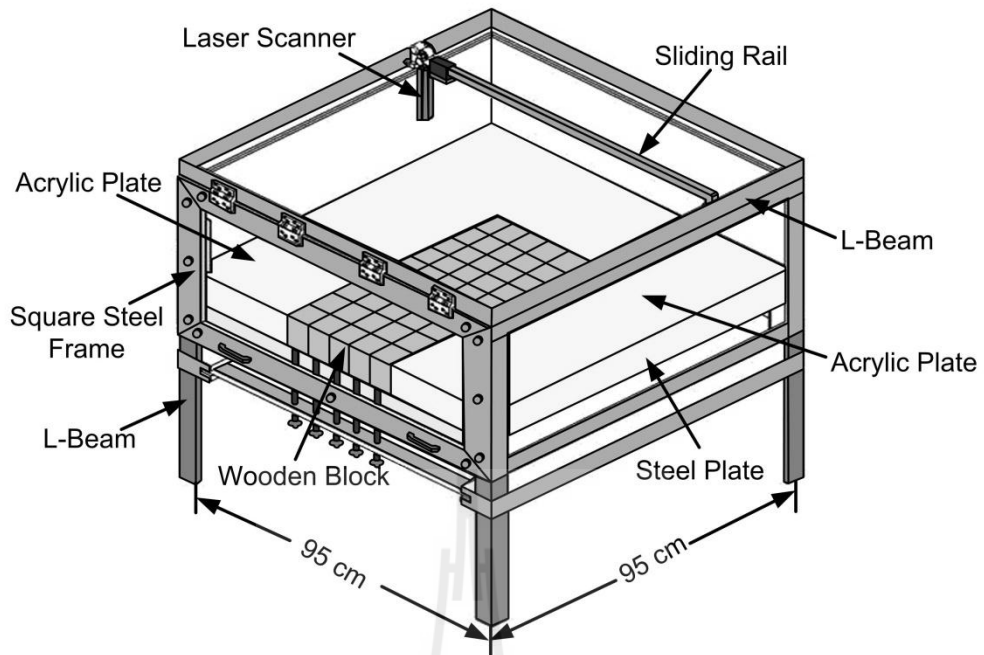


Figure 4.2 Perspective view of trap door apparatus.

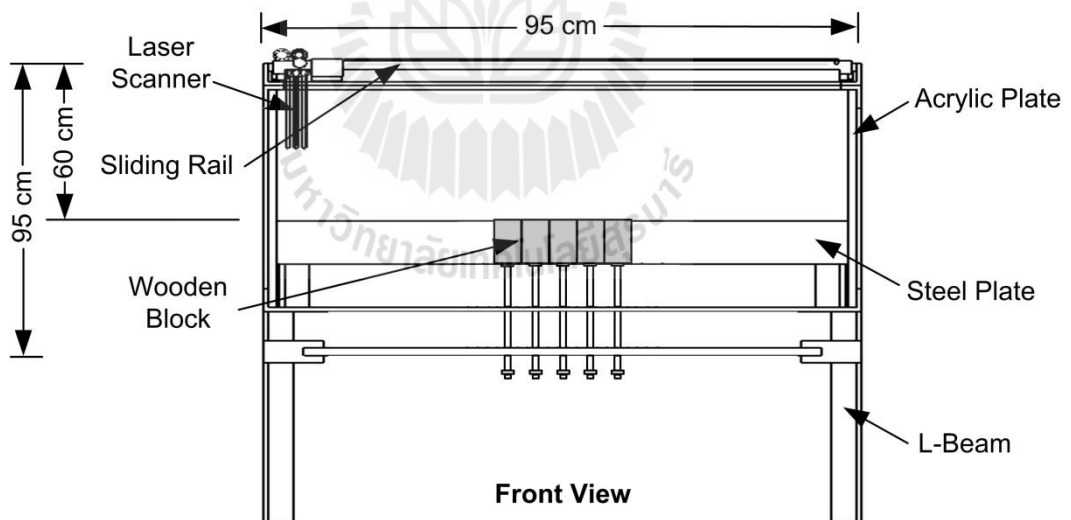


Figure 4.3 Front view of trap door apparatus.

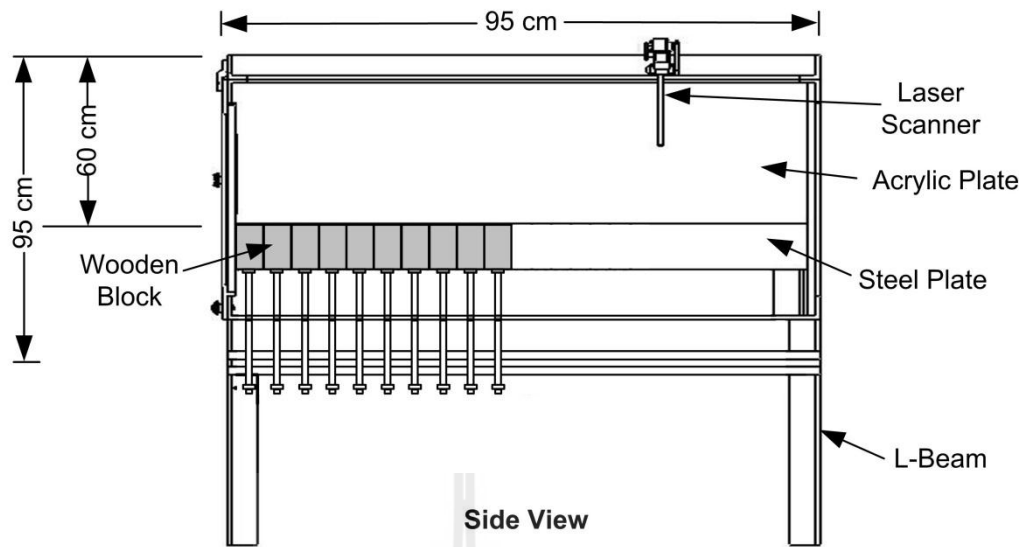


Figure 4.4 Side view of trap door apparatus.

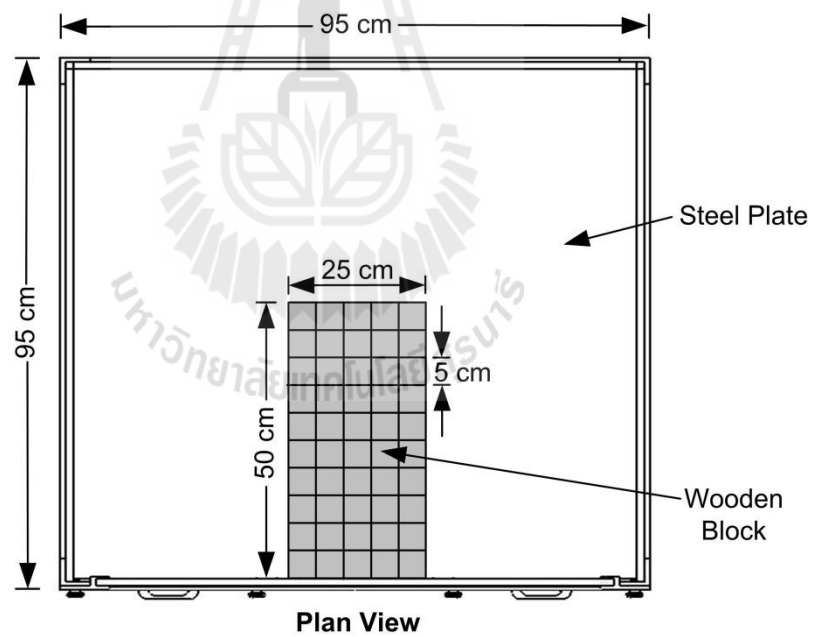


Figure 4.5 Plan view of trap door apparatus.

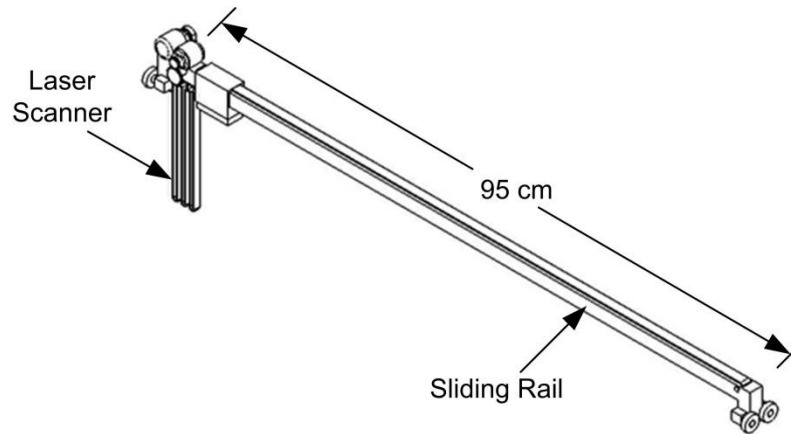
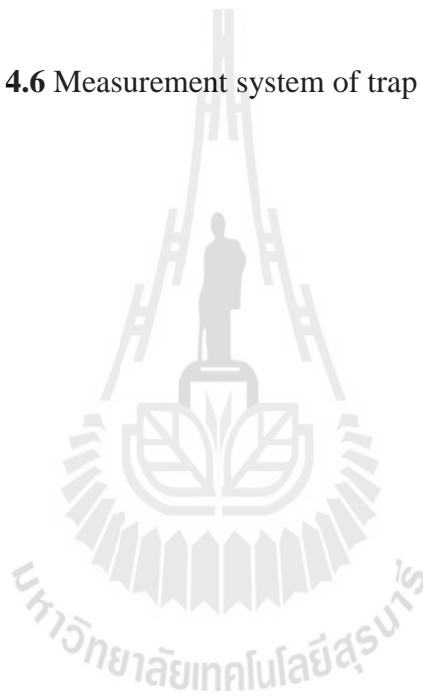


Figure 4.6 Measurement system of trap door apparatus.



CHAPTER V

PHYSICAL MODEL SIMULATION

5.1 Introduction

Physical modeling has played an important role in studies related to stability of underground mines and tunnels. A variety of modeling techniques has been developed all over the world to study ground response to underground excavation and tunneling. The objective of the physical model testing in this study is to assess the effects of underground opening geometries and block size of the overburden on surface subsidence. The laboratory testing is performed to reveal the maximum magnitude of subsidence (S_{\max}) and the angle of draw (γ), and hence allowing to study the effect of opening geometries and mechanical properties of overburden.

5.2 Physical model testing

Physical model simulations have been performed to determine the effects of underground opening configurations (widths, lengths, heights and depths) and block size of the overburden on surface subsidence under super-critical conditions. This study indicates the importance of the main factors that control the extent of subsidence produced on the surface and determines the effects of geometry of underground openings on the angle of draw, the maximum subsidence and the volume of the subsidence trough. Three size ranges of clean and uniform granular materials with selective sizes (2, 4.75 and 12.5 mm) are used to simulate individual blocks in

overburden. A trap door apparatus used to represent the scaled-down three-dimensional simulations of surface subsidence which allows fully controlled test conditions. The underground opening is simulated by systematically pulling down the wooden blocks underneath the sample container. The opening width (W) can be simulated from 50 mm to 250 mm with an increment of 50 mm. The opening length (L) can be simulated from 50 mm up to 250 mm with 50 mm increment. The opening height (H) is selected from 10, 20, 30, 40, to 50 mm. The overburden thickness (Z) is varied from 50 to 200 mm.

In this study, the opening width (W) is maintained constant at 5 cm. The block size-to-opening width ratios (B_s/W) are varied from 0.06, 0.10 to 0.25 for the gravel particle sizes at 2.0, 4.75 and 12.5 mm, opening depth-to-width ratios (Z/W) from 1, 2, 3, 4 to 5, opening height-to-width ratios (H/W) from 0.2, 0.4, 0.6, 0.8 to 1, and opening length-to-width ratios (L/W) from 1, 2, 3, 4 to 5. Figure 5.1 shows the test parameters and variables defined in the simulations. All blocks equivalent to the predefined W and L are simultaneously moved down. The effect of the mining sequence is not investigated in this paper. For each series of simulations the sample container is filled with the materials to a pre-defined thickness. The thickness of the material layer represents the opening depth or the thickness of overburden. The material is lightly packed and the top surface is flattened before beginning the test. Each opening configuration is simulated at least 3 times to verify the repeatability of the results.

While the underground opening is simulated, the settlement of the top surface of the granular materials occurs. The laser scanner measures the surface profile of the overburden before and after the subsidence is induced. An example of a scanned

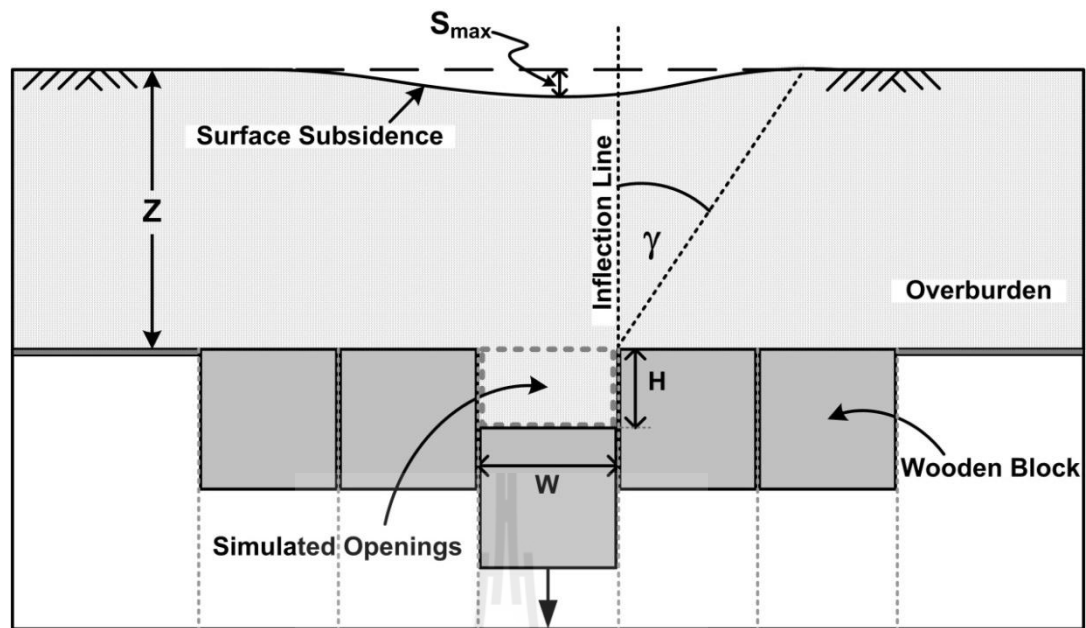


Figure 5.1 Variables used in physical model simulations and analysis.

image under various the opening lengths are shown in Figure 5.2. The simulation results are focused on the variation of the angle of draw and the maximum surface subsidence as affected by the opening geometry block size and frictional resistance of the gravel particles.

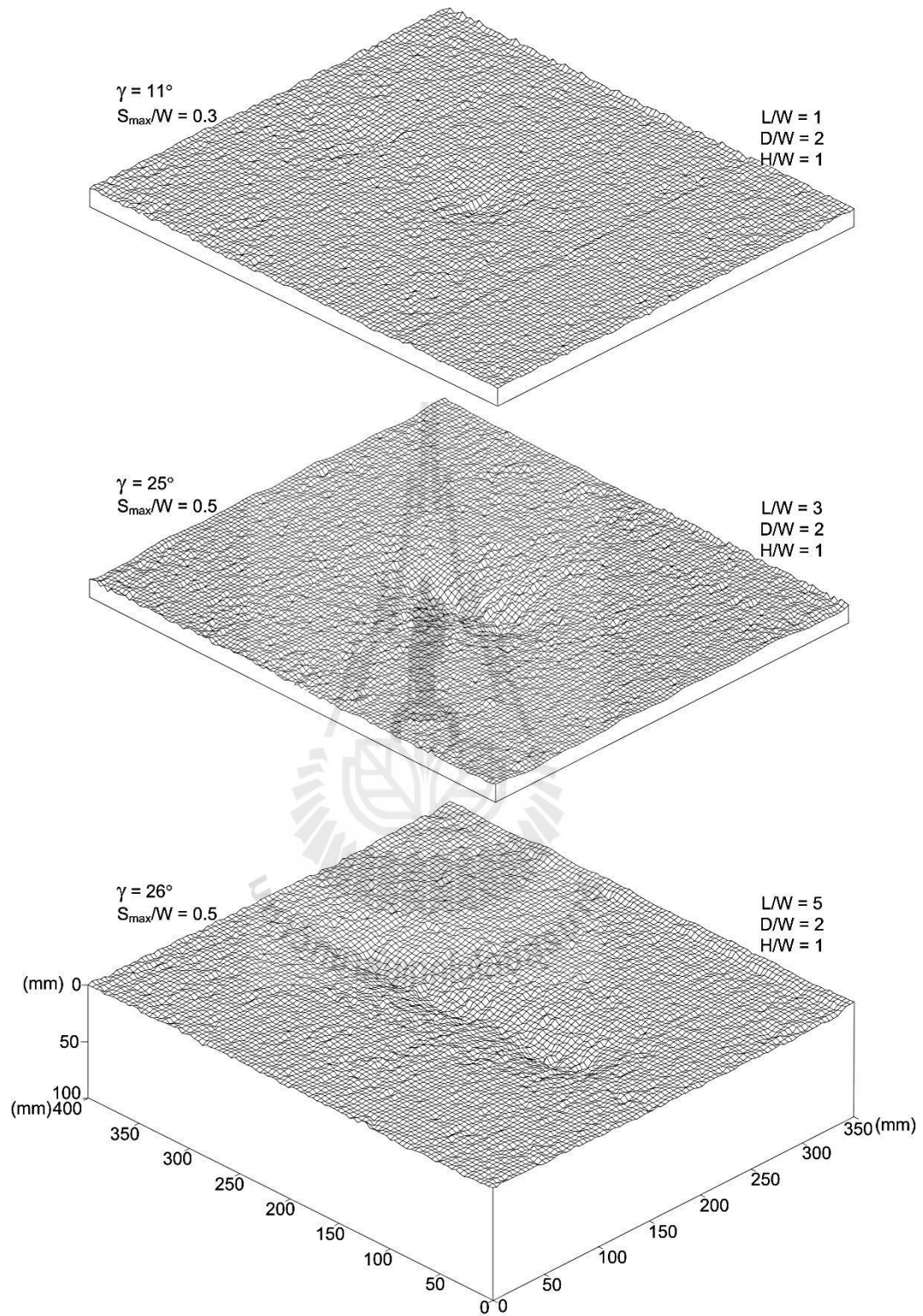


Figure 5.2 Example of three-dimensional laser scanned image of surface subsidence.

5.3 Test results

Super-critical subsidence usually occur where the mine depth is less than the width of the mined-out area. This type of subsidence is induced by the shallow mining, and affects the ground surface substantially. Collapse of cavern roof and overburden can occur when the subsidence reaches its super-critical condition, which is dictated by the cavern height. If the cavern height is equal to or less than the roof deformation, the immediate roof rock will touch the cavern floor. If the cavern height is however significantly greater than the critical roof deformation, failure of the cavern roof can occur under the super-critical condition. The failure can progress upward and leads to a sinkhole development.

The results obtained here are presented in terms of the angle of draw (γ) and the maximum subsidence (S_{\max}). The angle of draw is a parameter used for defining the position of the limit of subsidence at the surface. The angle of draw is the angle between a vertical line from the edge of the underground opening and a line from the edge of the opening to the point of zero surface subsidence (Figure 5.3). The point of maximum surface subsidence is located in the center of the trough.

Figure 5.4 shows the angle of draw as a function of the opening length-to-width ratio (L/W). The angle of draw increases with increasing L/W ratio and tends to approach a limit when L/W is beyond 3. This is probably because the effect of the opening ends decreases and eventually disappears when the L/W is beyond 3. Figure 5.5 shows the angle of draw as a function of the opening height-to-width ratio (H/W). The results indicate clearly that the angle of draw increases with increasing H/W ratio. This is because under super-critical conditions, the material can collapse (flow) into the opening more and induce larger angle of draw and trough width. Under the same

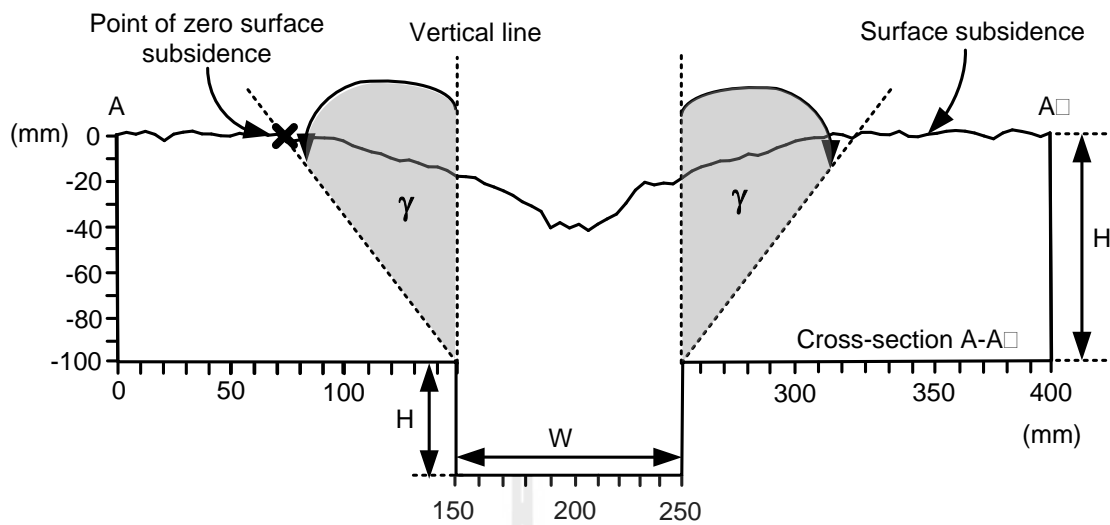


Figure 5.3 Definition of angle of draw.

L/W and H/W ratios, increasing the Z/W ratio can reduce the angle of draw (Figure 5.6). This is due to that the settlement in the physical model has created new voids in the overburden above the opening.

The maximum subsidence-to-opening width ratio increases with increasing L/W ratios (Figure 5.7). The maximum subsidence however tends to be independent of the opening length, when L/W is 2 or greater because the effect of the opening ends is reduced. The S_{\max}/W ratio increases with increasing H/W ratio (Figure 5.8) because the material can collapse into the opening more when the volume of opening becomes larger, particularly for $Z/W = 1$ (Figure 5.8(a)). The maximum subsidence tends to decrease as the opening depth increases (Figure 5.9). This is because of the inter-locking of gravel particles above the opening.

The subsidence of granular material (non-cohesive soils) is contingent on the granulometric composition, grain shape and grain roughness above the opening. The angularity and the particle size of the overburden can affect to the surface subsidence

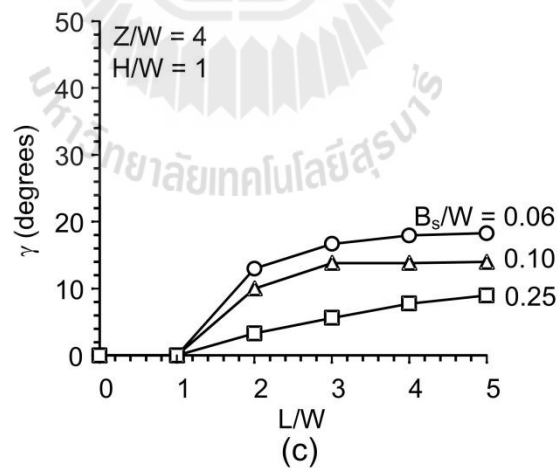
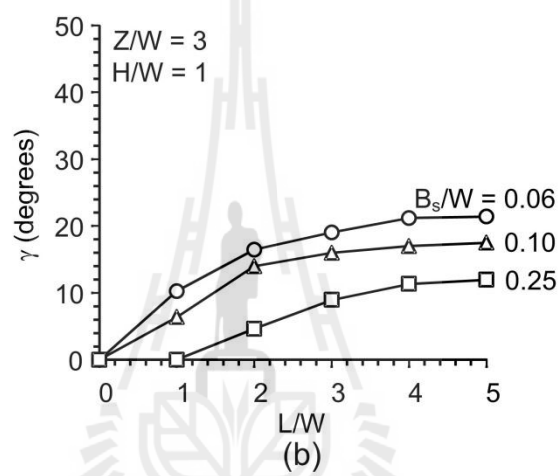
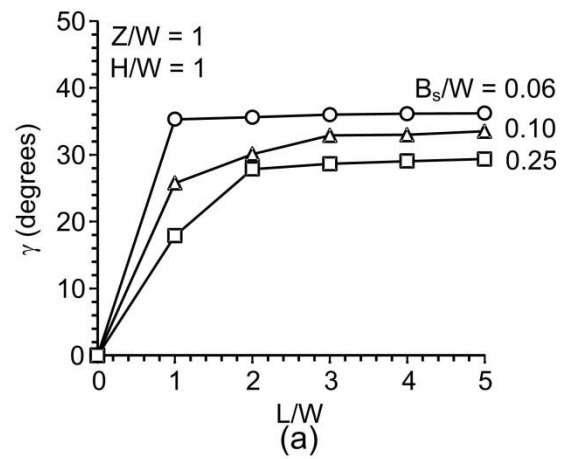


Figure 5.4 Angle of draw as a function of the opening length-to-width ratio.

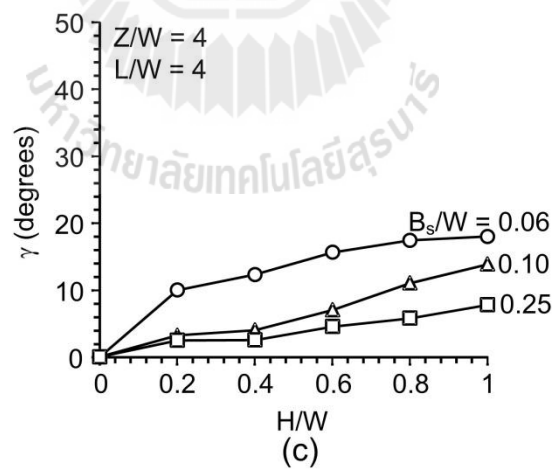
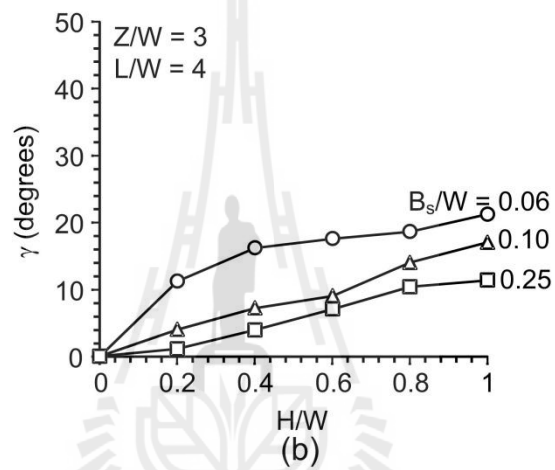
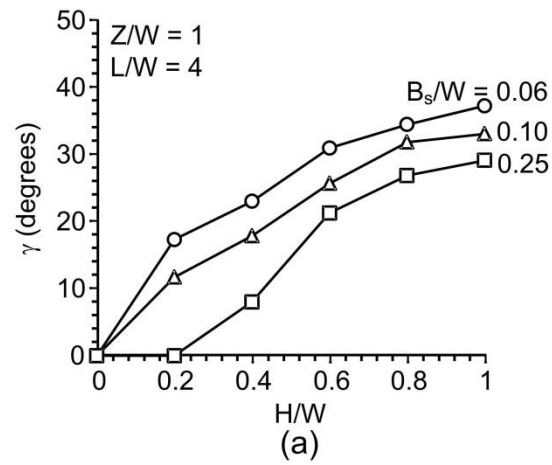


Figure 5.5 Angle of draw as a function of the opening height-to-width ratio.

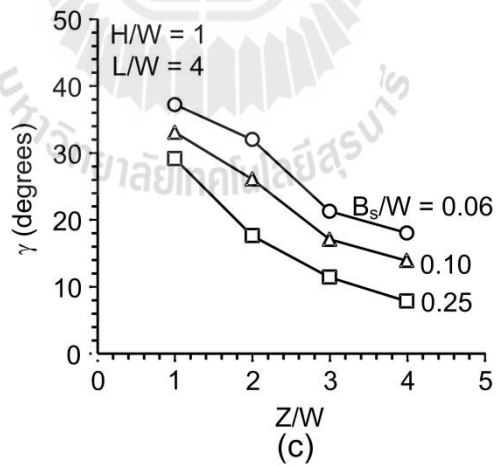
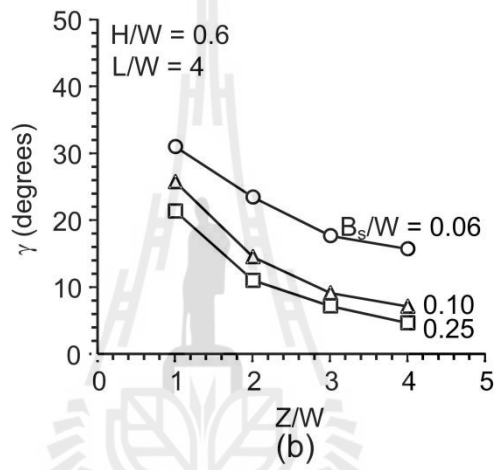
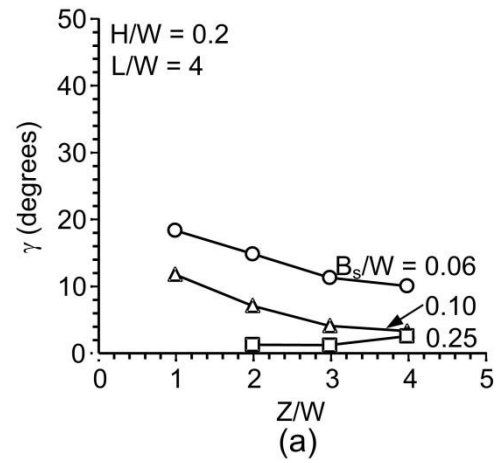


Figure 5.6 Angle of draw as a function of the opening depth-to-width ratio.

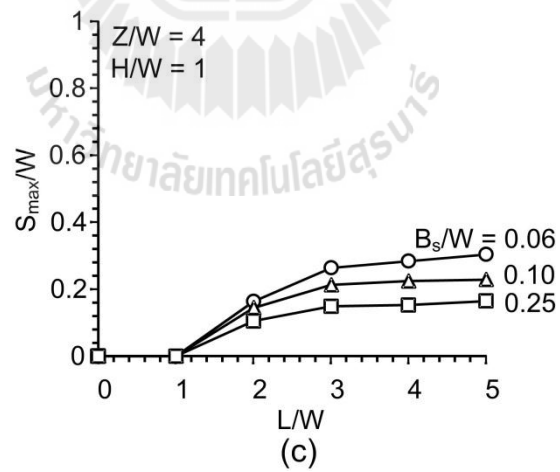
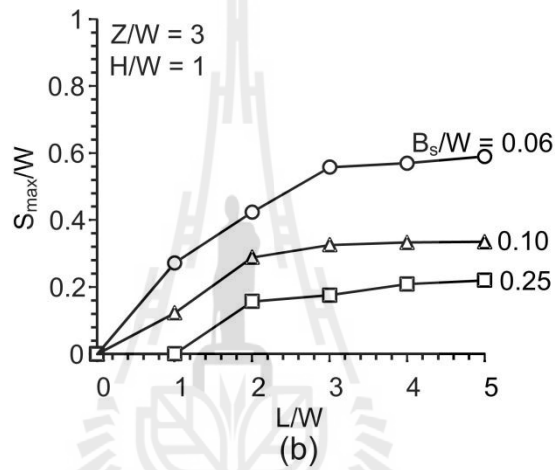
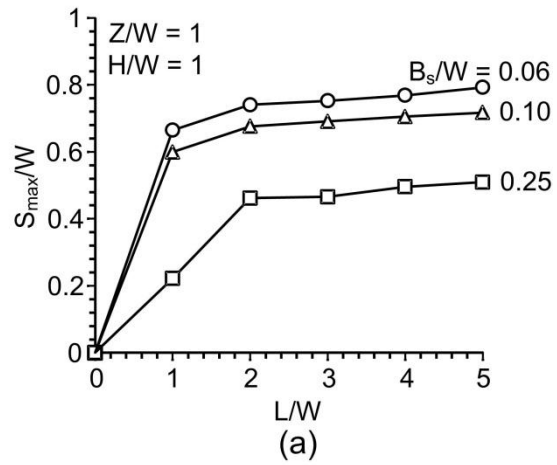


Figure 5.7 Maximum subsidence as a function of the opening length-to-width ratio.

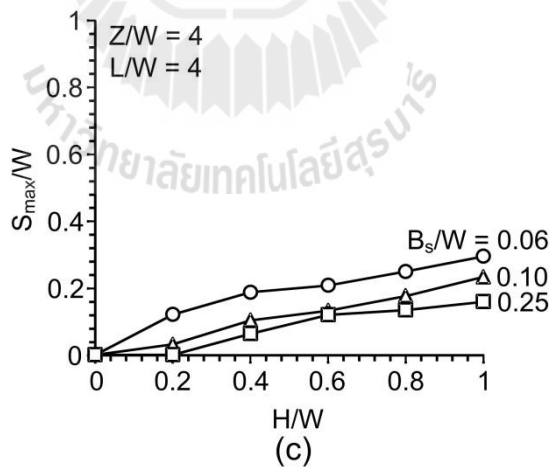
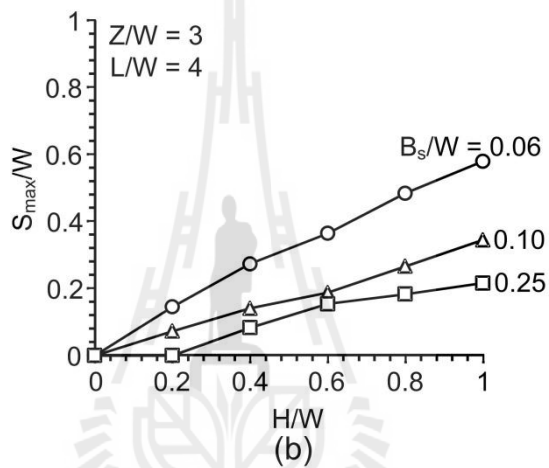
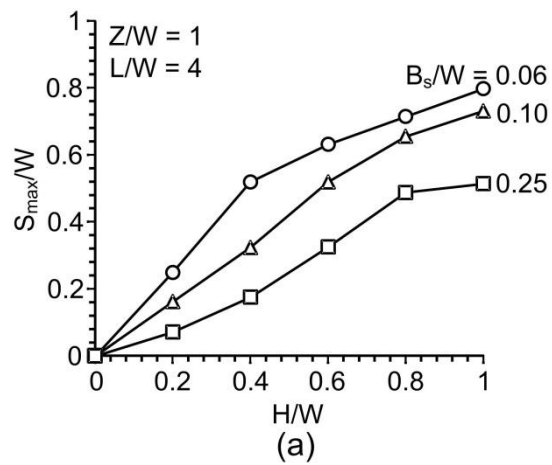


Figure 5.8 Maximum subsidence as a function of the opening height-to-width ratio.

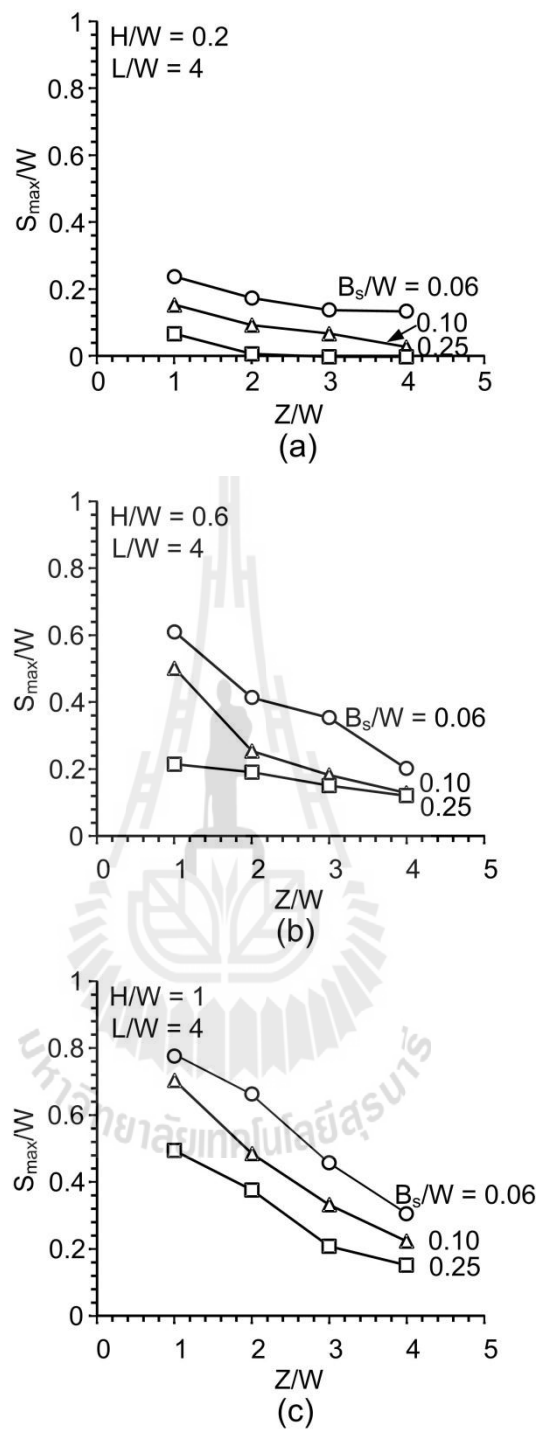


Figure 5.9 Maximum subsidence as a function of the opening depth-to-width ratio.

magnitude and volume. This is because of the inter-locking of gravel particles above the opening during flowing of particles. The surface subsidence is less when particles of overburden have more angularity and larger particle size.

To evaluate the effect of particle size, a series of block size are performed considering. The γ and the S_{\max}/W ratio decrease with increasing of block size or particle size (B_s/W ratios) for all cases (Figures 5.4 through 5.9). This agrees with numerical simulation by Yao et al. (1991). This is because smaller particles tends to move easier than the large ones. The larger particles tend to interlock above the opening. The surface subsidence is less when particles of overburden have more angularity or larger particle size. This is identified by the test results of Sakulnitichai et al (2009). They found the maximum span increases with decreasing joint spacing.

Particle size is one of the important properties which plays a dominant role on the stress, strain and strength responses of granular materials. Alteration of grain size results in the change of void ratio as well as particle effective contact area revolutionized and the load distribution mechanism of particle to particle contact (Islam et al., 2011). These changes directly affect to the volume of surface subsidence.

CHAPTER VI

EMPIRICAL SUBSIDENCE CALCULATION

6.1 Introduction

Empirically derived relationships are one of the principal methods of predicting mining and tunneling subsidence. This technique is based on the experience gained from a large number of actual field measurements. The empirical methods are quick, simple to use, and yield fairly satisfactory results. In this study, the laboratory test results are compared with subsidence profile predictions obtained from empirical methods for tunnels in fractured rock mass.

6.2 Previous studies on settlement trough

Other empirical or quasi-empirical methods have been proposed recently (Verruijt and Booker, 1996; Loganathan and Poulos, 1998) that show good correlations between observations from actual tunnels and predictions. Empirical methods, however, have significant shortcomings: (1) they have been developed or have been validated from a limited number of cases; (2) they should be applied only to tunnels that fall within the scope of the cases from which the method was developed; (3) only few soil and geometry parameters are taken into account; (4) they do not consider construction methods; and (5) they cannot give the complete solution of a tunnel with support. Empirical methods are still widely used; however, predictions of ground movements based on such methods are insufficient for most practical applications. There are a limited number of analytical and numerical tools

that can be used to predict ground deformations, but there is a growing demand for developing practical rational methods for tunnel design. Peck (1969) (See also McCusker, 1982; Monsees, 1996) established an empirical method for calculating surface settlements due to tunneling. Based on data from over twenty case histories, his results showed that the settlements above a tunnel are approximately symmetrical about the vertical axis of the tunnel. Peck showed that the short-term transverse settlement trough in a 'greenfield' could be approximated by a normal probability or error function curve. Although the use of this curve has no theoretical justification, it provides a method for estimating the settlements at varying distances from the centerline of the tunnel. Peck's investigation provides a guideline for the prediction of ground loss and settlement that occur in connection with tunneling.

While Peck (1969) saw no theoretical justification for the description of surface subsidence by means of an error function, others, in particular Litwiniszyn (1965, 1966) derived this subsidence function based on the random 'walking' of particles into a void space created underground. The Gaussian distribution curve has been used very widely in Eastern Europe for a very long time for the calculation of surface subsidence induced by mining (e.g. Martos, 1958 and Kratzsch, 1983, who give many more references). Scheidegger (1966) demonstrated that the Litwiniszyn derivations could be generalized, reducing the assumptions required. In recent years the stochastic approach has found renewed interest, notably within the context of discrete particle simulations of granular flow (e.g. Vairaktaris and Stavropoulou, 2013; Désérable, 2002).

6.3 Comparisons of subsidence trough profiles

The pertinent properties of the error function and its relationships to the dimensions of the tunnel are shown in Figure 6.1. R is the radius of the (circular) tunnel, and Z is the depth to the center of the tunnel. The maximum ordinate of the curve is the empirically determined maximum settlement S_{\max} . The points of inflection of the error curve are located at distance i on either side of the center line. If the value of i can be established, any table of the ordinates of the normal probability curve can be used to establish the ordinates at any other distance.

The empirical method given by Peck (1969) is used to predict the subsidence trough profile. Results obtained from this empirical method are compared with the physical simulation results.

Peck's equation representing the assumed trough shape is:

$$S = S_{\max} \exp(-x^2/2i^2) \quad (6.1)$$

where S is the surface settlement, S_{\max} is the maximum vertical settlement, x is the transverse distance from the tunnel centerline, and i is a measure of the width of the settlement trough, defined as the distance from the center to the point of inflection of the curve (corresponding to one standard deviation of the normal distribution curve), and is determined by the ground conditions.

Various expressions have been proposed for calculating the trough width at inflection point (i) as given in Table 6.1. Peck (1969) proposes that depth of the opening Z_c is measured from the gravel surface to the mid-height of the opening. However, it is found here that a closer agreement between the test results and the

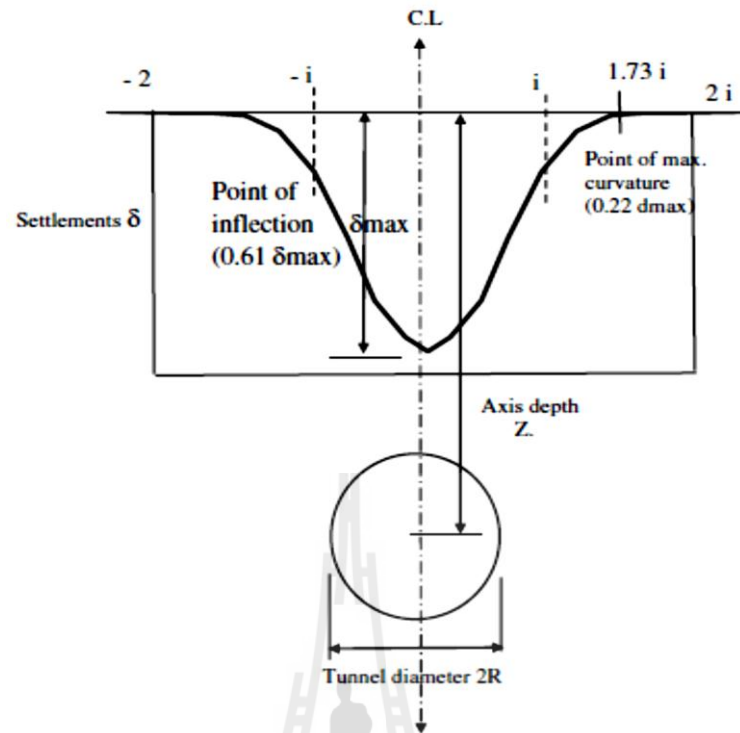


Figure 6.1 Properties of error function curve to represent cross-section settlement trough above tunnel (Adapted from Peck, 1969).

Table 6.1 Empirical solutions for estimation of settlement trough width.

Author	Width of settlement trough, i	Basis for empirical solution
O'Reilly and New (1982)	$i = 0.28Z - 0.1$ m (granular soil) $i = 0.43Z + 1.1$ m (cohesive soil)	Field observations of UK tunnels
Rankin (1988)	$i = k \cdot Z$ ($k = 0.25$ for cohesionless soils, $k = 0.50$ for clay)	Field observations

predictions was obtained if the depth is measured to the roof of the opening, as show in Figure 6.2. As a result this study will consider Z_r as the depth to opening roof.

Rankin (1988) and O'Reilly and New (1982) provide empirical solutions for “ i ” for both cohesionless material and cohesive soil. Their solutions are used here to compare with the settlement profiles obtained from the physical model simulations. The results indicate that the solutions of Rankin (1988) and O'Reilly and New (1982) for cohesive soil overpredicted the settlement trough measured from the physical model simulation, while their solutions for cohesionless soils is in good agreement with the measurement results. Figure 6.3 shows the settlement trough profiles predicted by different solutions of Rankin (1988) and O'Reilly and New (1982). The good agreement is obtained for $Z/W = 2, 3$ and 4 , while for $Z/W = 1$, the predicted trough profiles are smaller than the physical model results, as shown in Figure 6.4. Table 6.2 gives the parameter “ i ” and their corresponding coefficients of correlation for the simulations mentioned above.

6.4 Volume of surface settlement

Until the 1970s, not much data concerning ground movements above tunnels had been obtained. Since then, the available information has increased, primarily because of measurements and observations on the Baltimore and Washington, D.C. subway systems. These studies have defined the following terms:

- Volume change (ΔV). Increase or decrease in soil volume caused by the tunneling.
- Volume of surface settlement (V_S). The volume of the settlement trough at the ground surface.

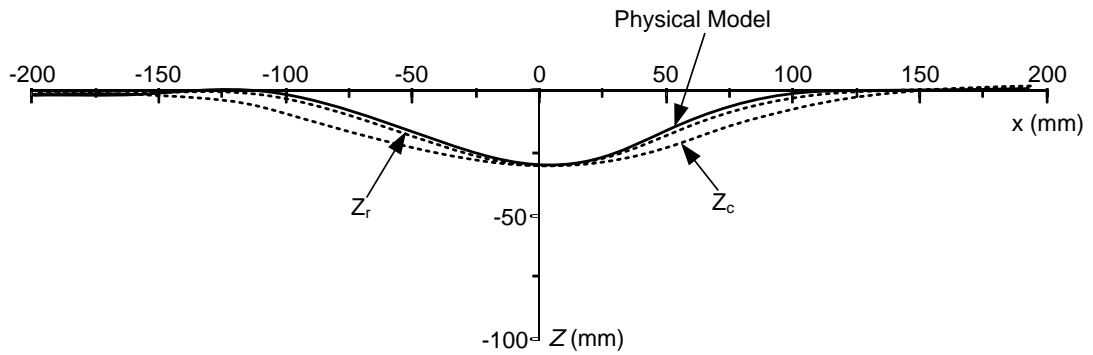


Figure 6.2 Comparison of the surface settlement trough calculations using values of Z_r and Z_c for $B_s/W = 0.10$, $H/W = 0.5$ and $L/W = 2$.

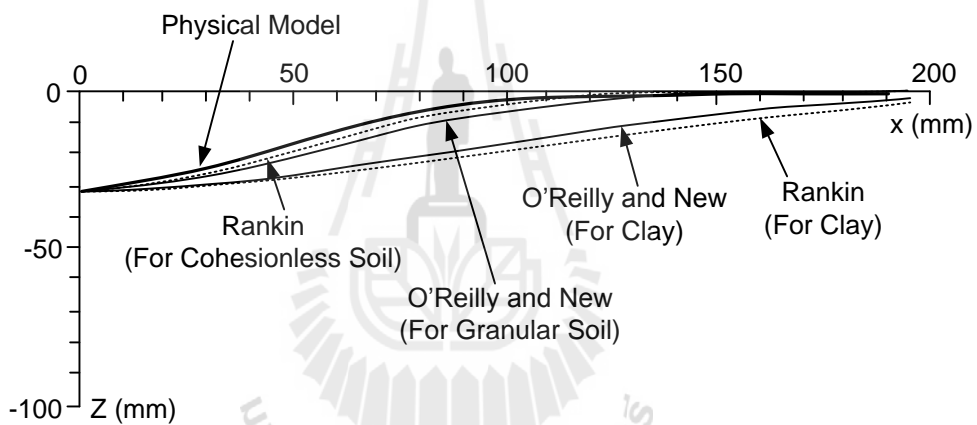


Figure 6.3 Example of comparison of the model simulation subsidence trough and the troughs calculated by different empirical formulae, where $B_s/W = 0.10$, $Z_r/W = 2$, $H/W = 0.5$ and $L/W = 2$.

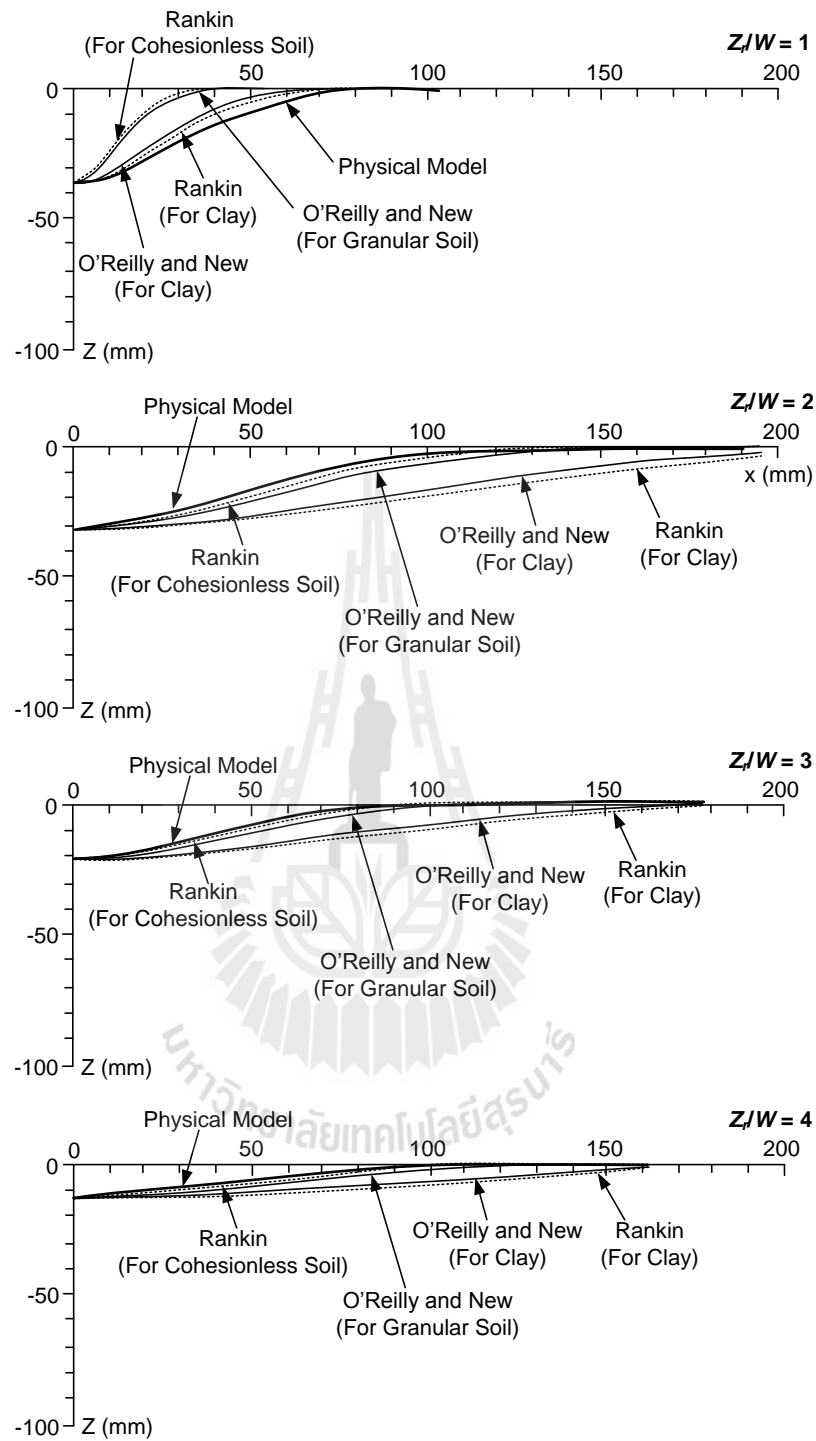


Figure 6.4 Surface settlement troughs for different values of Z_r/W where $B_s/W = 0.10$, $H/W = 1$ and $L/W = 5$.

Table 6.2 Estimation of the settlement trough width using different approaches when

$$B_s/W = 0.10, Z_r/W = 2, H/W = 0.5 \text{ and } L/W = 2.$$

Author	Width of settlement trough, i (mm)	R^2
O'Reilly and New (1982)		
- Cohesive soil	87.10	0
- Granular soil	55.90	0.789
Rankin (1988)		
- Clay	100	0
- Cohesionless soil	50	0.867

- Volume of lost ground (V_L). The volume of all ground movements taking place about the tunnel.

$$V_S = V_L - \Delta V \quad (6.2)$$

The relationship among these three quantities is complex and incompletely defined. However, for most purposes it is usually possible to assume that the volume of surface settlement is equal to the volume of lost ground. This assumption is generally workable except in soils exhibiting significant increases in soil volume (bulking) or decreases in soil volume (consolidation).

For a single tunnel, the volume of surface settlement for the individual tunnel is assumed equal to the volume of lost ground. Generally, the shape of the resultant settlement trough at the ground surface resembles that of the bell-shaped probability curve. This concept was used by Peck (1969) and others (Schmidt, 1979; McMuskler, 1982; Monsees, 1996) to correlate field measurements of trough width for several cases. In all cases in the calculations, the ground surface is assumed at the bottom of the building footing and the influence of building footing and building stiffness is

ignored. The volume of subsidence trough per unit length (V_s) is obtained from Peck's (1969) equation as:

$$V_s = 2.5 \cdot i \cdot S_{\max} \quad (6.3)$$

where S_{\max} is the maximum vertical settlement and i is the width of settlement trough, defined as the distance from the center to the point of inflection of the curve, which is obtained from Rankin's solution.

An attempt is made here to determine the effects of opening geometries on the volume of the subsidence trough. Figure 6.5 plots the subsidence trough volume normalized by the opening volume (V_s/V_o) as a function of opening height-to-width ratio (H/W), opening length-to-width ratio (L/W) and opening depth-to-width ratio (Z/W). The physical model results show clearly that the trough volume is less than the opening volume. This holds true for all opening geometries used here. The largest trough volume is obtained for $B_s/W = 0.06$ (smallest particles size) for all cases. This is because of the inter-locking of gravel particles above the opening during flowing of particles. The V_s/V_o ratios are greater if finer gravels are used in the simulation. This is due to the angularity and the particle size of the overburden can significantly affect to the surface subsidence magnitude and volume. The small particles size has been obtained the effect of the angularity less than the large size. The subsidence trough volume tends to decrease as the opening height (Figure 6.5(a)) and opening depth increase (Figure 6.5(c)) because the physical model has created new voids above the opening, and trough volume eventually constant when the L/W is beyond 3 (Figure 6.5(b)).

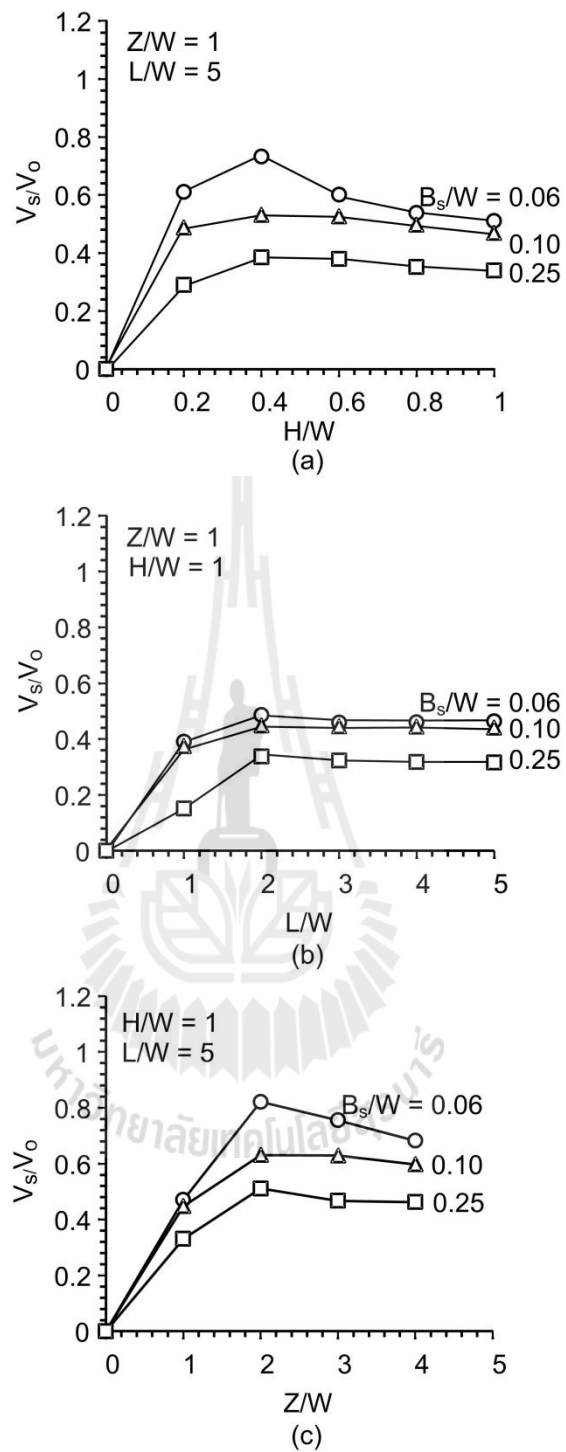


Figure 6.5 Volumetric ratios as a function of opening height ratio (a), opening length ratio (b) and opening depth ratio (c).

CHAPTER VII

NUMERICAL ANALYSIS

7.1 Introduction

This chapter describes the discrete element analyses performed by using Particle Flow Code (PFC^{2D}-Itasca, 2008) to simulate the surface subsidence profile correlated with the overburden mechanical properties and underground opening configurations. The results obtained from the PFC^{2D} are compared with the physical models simulations.

7.2 Discrete element analyses

PFC^{2D} simulates the movement and interaction of circular particles by the distinct element method (DEM). The original application of this method was as a tool to perform research into the behavior of granular material; representative elements containing several hundred particles were tested numerically. The particle model was used to understand element behavior (in which conditions are “uniform”), and a continuum method was used to solve real problems that involve complicated deformation patterns (with the element behavior derived from the particle-model tests). In this study, discrete element analyses are performed to compare the results with those of the physical models.

The walls are generated in order to be used to simulate the boundary conditions of the overburden and the underground opening. All walls of the models are considered smooth and nonrestrictive with regards to material movement. The

boundary conditions used in the simulation are identical to those of the physical model tests.

The generate command placed particles within the boundary specified such that no overlap occurs. The tries keyword specified 400,000 attempts to add the desired number of particles within the defined area. It simply created the desired underground mining region and increased the number of tries to fit all of the particles within the specified area. This method is slow to achieve the initial equilibrium state, since particles move large distances to come to rest of overburden. Once all of the particles were at rest and the model was at equilibrium, the top of the particle assembly is leveled by deleting all particles above a specified thickness of overburden (Figure 7.1).

The command codes define the generation of the overburden model and the boundaries, as well as perform the extraction operations similar to those in the physical models. Each particle is assigned by the same property values as those of the physical granular materials. The material properties of the PFC^{2D} models are shown in Tables 7.1. After the particles are at rest and the model is at equilibrium as predefined overburden thickness, the wall above the opening (roof) is deleted for simulation the extraction of material from each case using the equivalent procedures used in the physical model. The particles are continuously flowed into the opening floor until the opening completely filled and hence the surface subsidence is induced (Figure 7.2). Each numerical model has a processing of approximately 20,000-40,000 cycles until each particle is not flowing and moving. The subsidence of overburden, both physical and numerical, was governed by gravity.

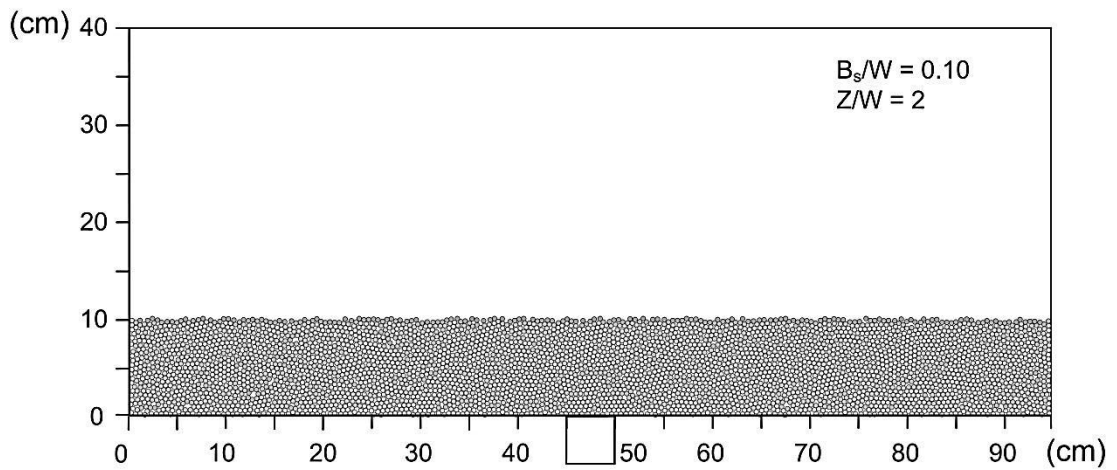


Figure 7.1 Surface subsidence before the opening simulation with predefined overburden thickness.

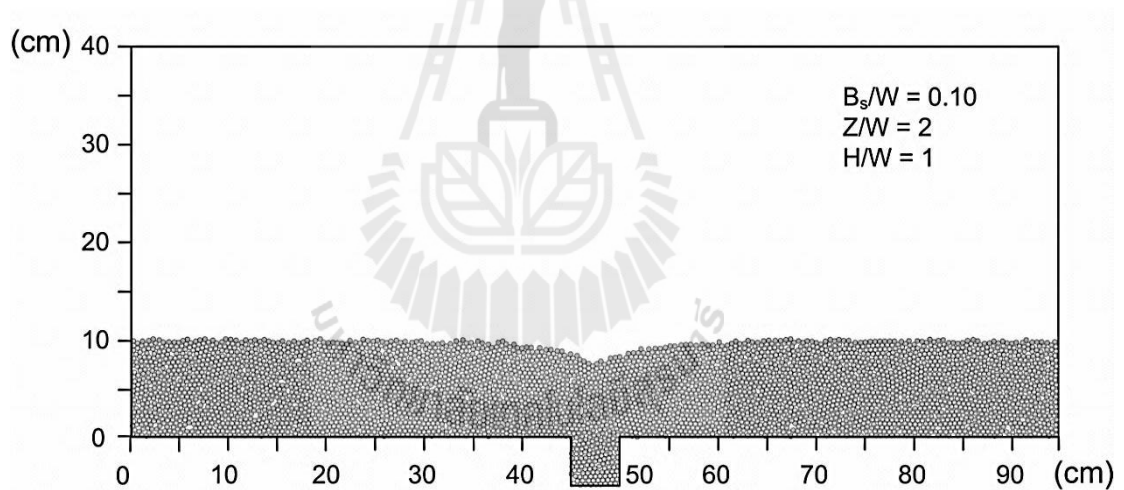


Figure 7.2 Example of PFC^{2D} model for surface subsidence after the opening simulation.

Table 7.1. PFC^{2D} simulation parameters.

Particle size (mm)	Ball radius (mm)	Bulk density (kN/m³)	Friction coefficient (tan ϕ)	Normal stiffness, K_n (MN/m)	Shear stiffness, K_s (MN/m)
2.00	1.00	1455	0.46	44.54	0.73
4.75	2.38	1530	0.59	25.25	0.96
12.5	6.25	1567	0.68	17.30	1.28

Physically, each extraction removed the material in three dimensions. PFC^{2D} modeling, however, is limited to two dimensions. Although a three-dimensional version (PFC^{3D}) is available, it was not used in this study. Few cases have been studied in order to investigate the effect of underground opening geometries on the angle of draw and the maximum subsidence. The effects of opening length is assessed by simulating the L/W from 3, 4 to 5 and opening height H/W from 0.2 to 1, where W = 50 mm. The effect of opening depth is investigated by varying Z/W ratios from 1 to 4. The B_s/W vary from 0.06, 0.10 to 0.25 to study the effect of block size. The results obtained from PFC^{2D} simulations are compared with the physical model results under the opening length-to-width (L/W) ratio beyond 3 for reducing the problem of the missing dimension of opening lengths due to that the angle of draw and the maximum subsidence tend to be constant as the L/W ratio is sufficiently large.

The relationship between the angle of draw, maximum subsidence and the opening depth-to-width (Z/W) ratios has been examined and is illustrated in Figure 7.3. The results show that the angle of draw and the maximum subsidence decrease with increasing opening depth. Particle size is the property that plays a dominant role on the displacement responses of granular materials. Alteration of grain size results in the change of void ratio as well as particle effective contact area revolutionized and

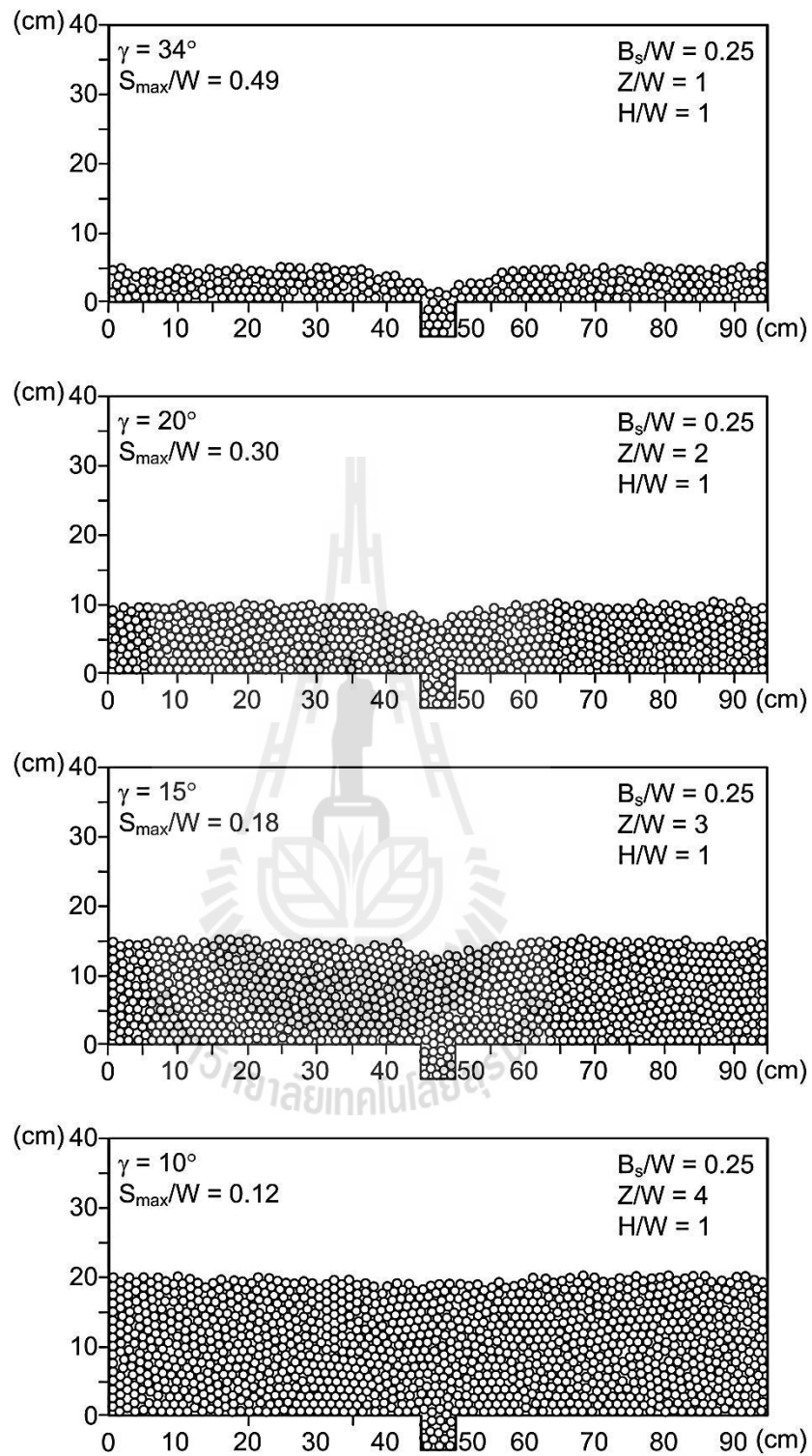


Figure 7.3 Surface subsidence under various opening depth-to-width (Z/W) ratios.

the load distribution mechanism of particle to particle contact. These changes directly affect to the volume of surface subsidence due to the inter-locking of gravel particles above the opening during flowing of particles. Figure 7.4 shows the arrangement characteristics of each particle size under the same underground opening geometry. The surface subsidence is less when particles of overburden have larger particle sizes.

According to the results of particles flow numerical simulation, some conclusions can be reached. When the underground opening is occurred, the particle immediately collapsed into the opening. The particles above the opening show cone of failure at the first step (Figure 7.5), and then the particles continuously flowed into the opening, eventually the surface collapsed, causing surface subsidence. Based on the surface subsidence mechanism of full extraction, the point of maximum surface subsidence is located in the centre of ground surface above the opening (Figure 7.2).

7.3 Comparison of numerical and physical models

After several trials, the angle of draw and the maximum subsidence can be determined for each opening configurations. The PFC^{2D} results are compared with those observed from the physical models in Figures 7.6 and 7.7 for various opening depths.

The PFC^{2D} simulations show the decreasing trends of the angle of draw with overburden thicknesses which are similar to those observed from the test models. For all cases the predicted angle of draw slightly over-estimates the test results (Figure 7.6). This is probably because the circular particles models in the discrete element analyses are perfectly shaped with identical joint properties while in the test models the gravels shapes are not perfect and the frictional strength is unlikely to be identical

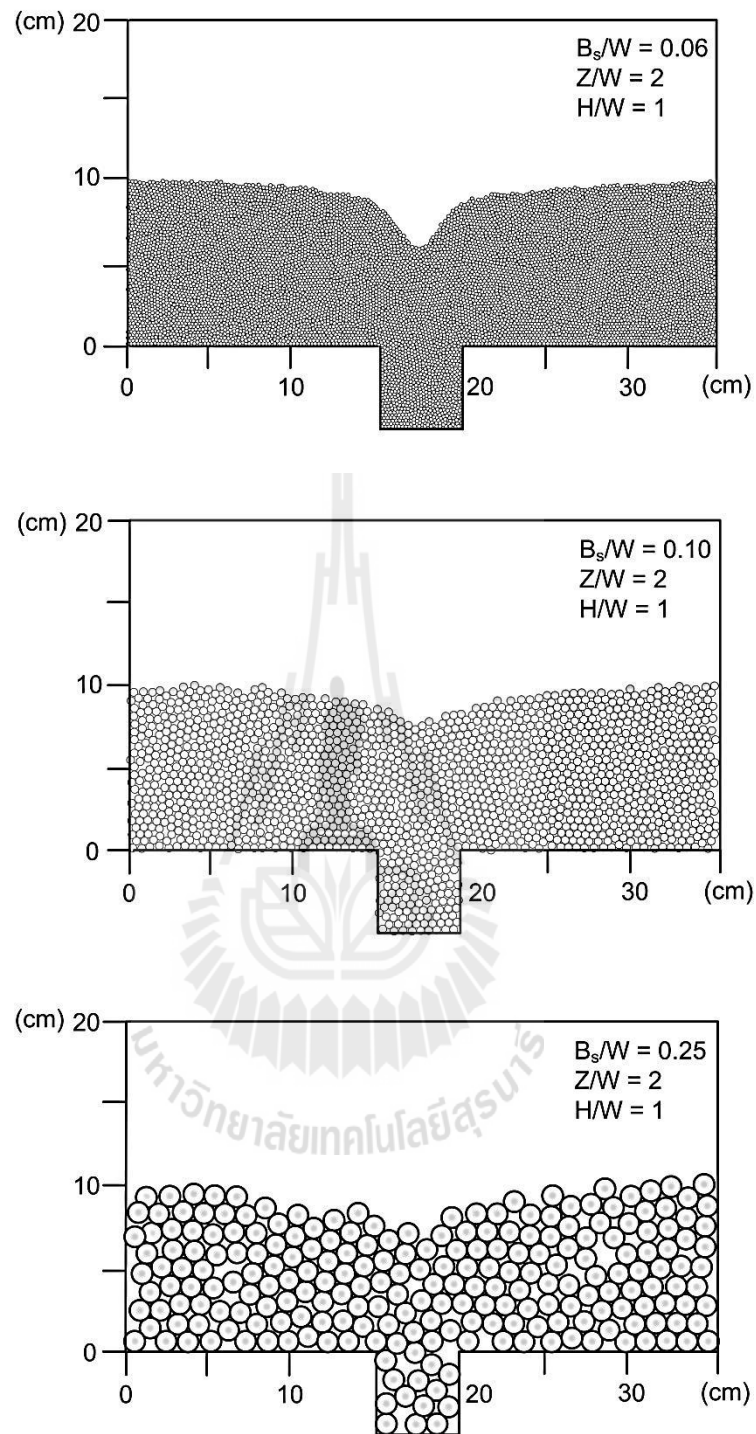


Figure 7.4 Characteristics of each particle size under the same underground opening geometry.

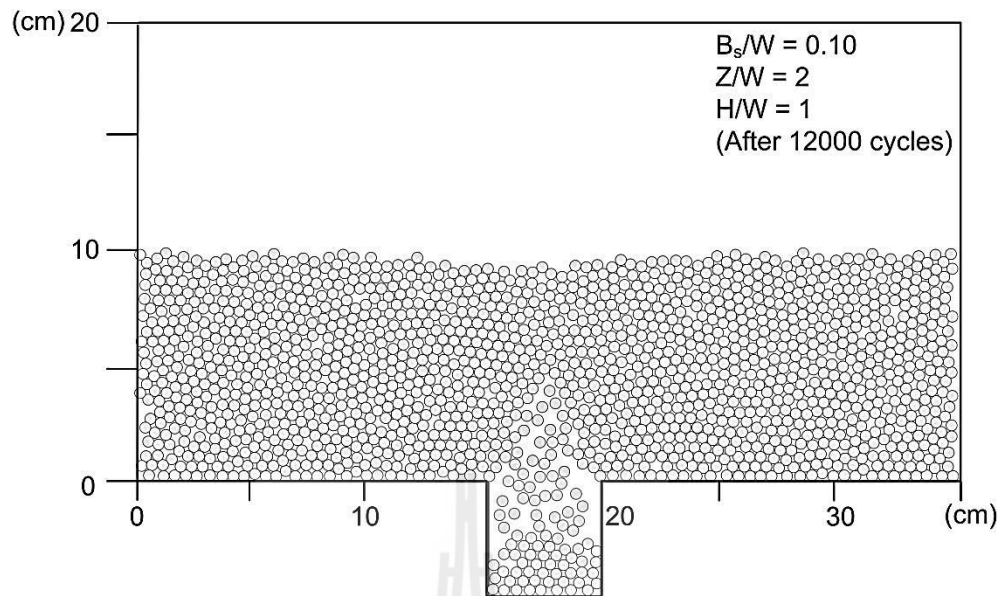


Figure 7.5 Failure characteristic on first step of the overburden after the opening simulation.

for all contacts (granular surfaces). The angularity and the particle size of the overburden also affect to the surface subsidence magnitude and volume. The interlocking of gravel particles during flowing in physical simulations more than found in the PFC^{2D}. As a result the circular particles constructed in the PFC^{2D} models can subsidence easier than those tested in the physical models, and hence yield a wider angle of draw (the extent of the surface subsidence are over). Figure 7.7 shows the maximum subsidence-to-opening width ratio (S_{\max}/W) decreases with increasing Z/W ratios in each particle sizes. For all cases the predicted maximum subsidence agrees well with the test results. From the results found that the numerical models can be extrapolated to predict the super-critical subsidence behavior of fractured rock mass.

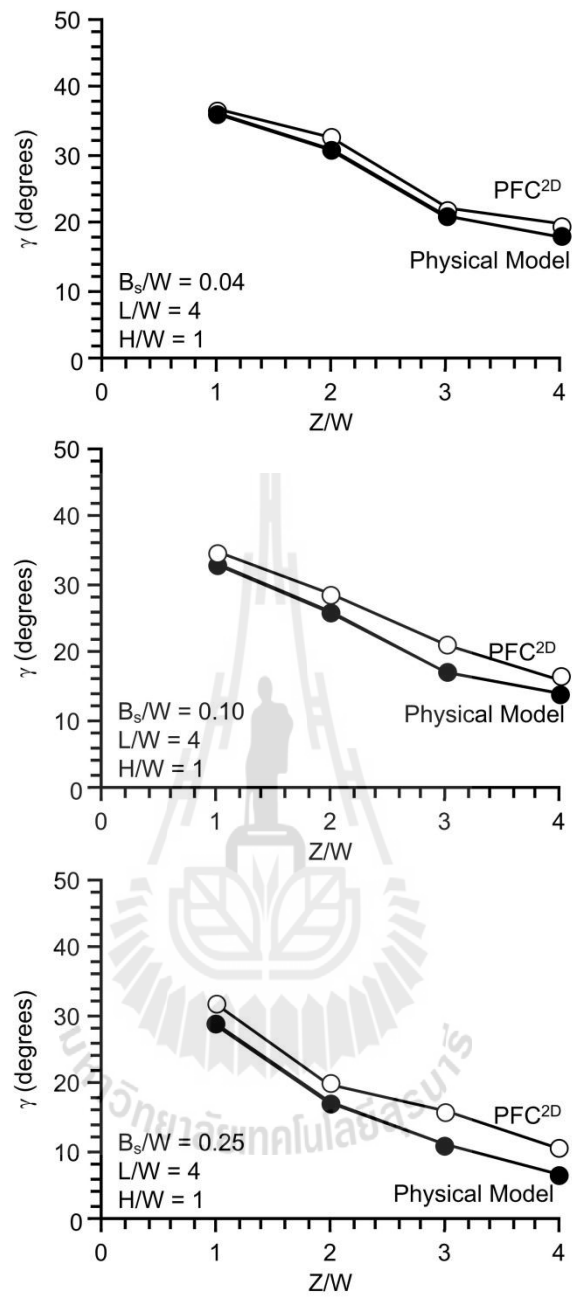


Figure 7.6 Comparisons of the angle of draw (γ) obtained from PFC^{2D} and physical model test.

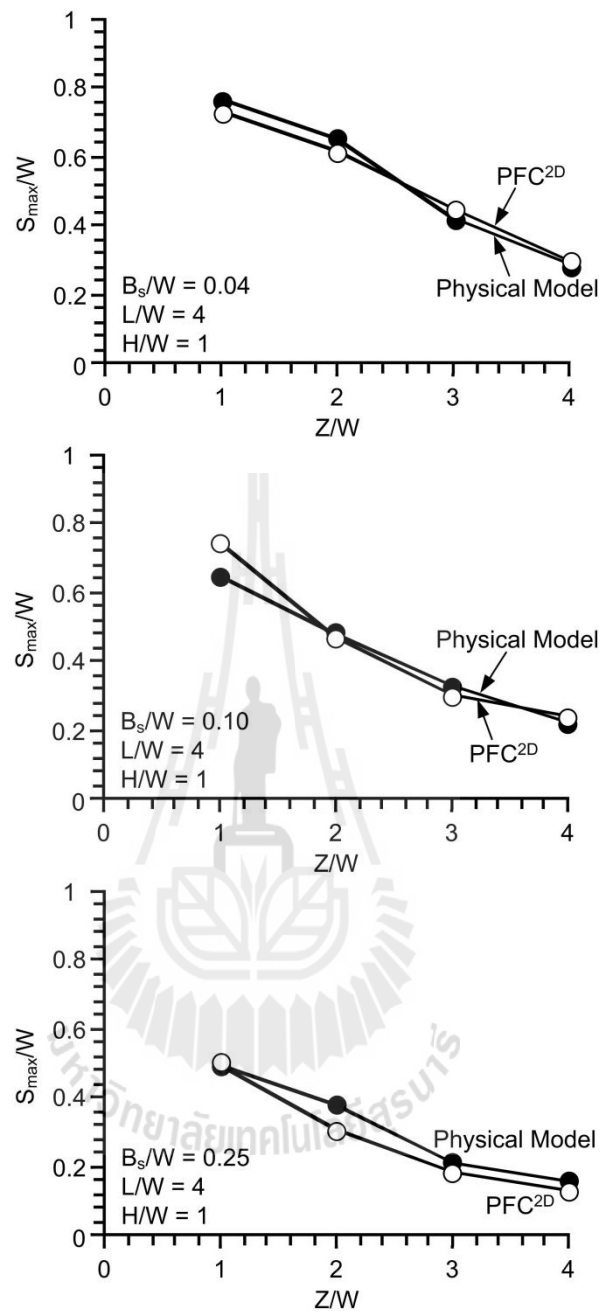


Figure 7.7 Comparisons of the S_{max}/W obtained from PFC^{2D} and physical model test.

CHAPTER VIII

DISCUSSIONS AND CONCLUSIONS

8.1 Discussions and conclusions

The effects of underground opening configurations and block size of the overburden are determined to predict the super-critical surface subsidence. The surface subsidence has been simulated using physical models, empirical calculations and numerical analyses. From the results the following conclusions can be drawn. The physical model results clearly indicate that the angle of draw and the maximum subsidence are controlled by the geometrical characteristics of underground openings, overburden thickness and the mechanical properties of the overburden. The extent of the mining subsidence affected area is defined by the angle of draw, which is controlled predominantly by geological conditions of the overburden strata and the mining configurations.

The angle of draw and maximum subsidence increase with increasing L/W ratio and tends to approach a limit when L/W is greater than 3. For the same underground opening geometry, increasing the Z/W ratio reduces the angle of draw and the magnitudes of maximum subsidence. The γ and S_{\max}/W ratio decrease with increasing block size or particle size of granular materials that are used to simulate the overburden.

The empirical solutions for cohesionless material provided by Rankin (1988) and O'Reilly and New (1982) fit well to the physical model results, particularly for

Z_r/W greater than 2. In general the results of our physical model simulation agree reasonably well with the conclusion drawn by Fattah et al. (2013) that Rankin's solution can provide the best production of the subsidence settlement profiles for cohesionless materials. However, to evaluate the width of the settlement trough, using the distance Z_r from surface to the roof of the underground opening gave better predictions than using the distance Z_c from the surface to the center of the tunnel.

The volume of subsidence trough observed from the physical model is always less than the opening volume. The largest trough volume is obtained for smallest particles size ($B_s/W = 0.06$) for all cases. This is because of the inter-locking of granular particles is reduced if the finer gravels are used in the simulation. The overburden angularity can also significantly affect to the surface subsidence magnitude and volume. The effect of the angularity is less for the smaller particles size. The subsidence trough volume tends to decrease as the opening height and depth increase because the physical model has created new voids above the opening, and trough volume eventually constant when the L/W is beyond 3. The subsidence trough volume decreases as the Z/W ratios increases beyond 3. The results of discrete element analyses agree well with those obtained from the physical models. The predicted angle of draw however slightly over-estimates the test results due to the PFC^{2D} cannot identify the effect of the angularity of particle which is different from the gravels shapes in the physical model. The numerical models can be useful to predict the super-critical subsidence behavior of fractured rock mass above mine openings, particularly when the block sizes are much less than the opening width.

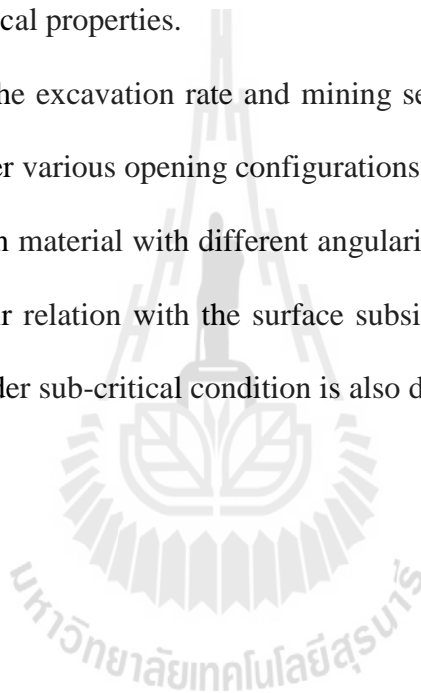
8.2 Recommendations for future studies

The scope of this study is relatively narrow. The uncertainties of the investigation lead to the recommendations for further studies.

The physical model simulations should be performed on a greater opening geometries ratio to confirm the effect of opening depth, width, length and height on surface subsidence extent. More simulation is also required on a variety of materials with different mechanical properties.

The effect of the excavation rate and mining sequence on surface subsidence should be studied under various opening configurations and overburden properties.

The overburden material with different angularities and particle shapes should be tested to study their relation with the surface subsidence. The knowledge of the surface subsidence under sub-critical condition is also desirable.



REFERENCES

- Aracheeploha, S., Horkaew, P., and Fuenkajorn, K. (2009). Prediction of cavern configurations from subsidence data. In **Proceedings of the Second Thailand Symposium on Rock Mechanics** (pp. 116-176). Chonburi: Suranaree University of Technology.
- Asadi, A., Shahriar, K., Goshtasbi, K., and Najm, K. (2005). Development of new mathematical model for prediction of surface subsidence due to inclined coal-seam mining. **Journal of the South African Institute of Mining and Metallurgy**. 105: 15–20.
- ASTM Standard D2487–06. (2006). **Standard Practice for Classification of Soils for Engineering Purposes (Unified Soil Classification System)**. Annual Book of ASTM Standards, American Society for Testing and Materials, West Conshohocken, PA.
- ASTM Standard D422–63. (2007). **Standard Test Method for Particle-Size Analysis of Soils**. Annual Book of ASTM Standards, American Society for Testing and Materials, West Conshohocken, PA.
- ASTM Standard D5607–08. (2008). **Standard Test Method for Performing Laboratory Direct Shear Strength Tests of Rock Specimens Under Constant Normal Force**. Annual Book of ASTM Standards, American Society for Testing and Materials, West Conshohocken, PA.
- Azéma, E., Estrada, N., and Radjai, F. (2012). Nonlinear effects of particle shape angularity in sheared granular media. **Physical Review E**. 86(041301): 1-15.

- Baghuguna, P.P., Singh, B., Srivastava, A.M.C., and Saxena, N.C. (1991). A critical review of mine subsidence prediction methods. **Mining Science and Technology**. 13(3): 369-382.
- Caudron, M., Emeriault, F., Kastner, R., and Al Heib, M. (2006). Sinkhole and soil-structure interaction: Development of an experimental model. In **International Conference on Physical Modeling in Geotechnics** (pp. 1261-1267). Hong-Kong.
- Dai, H., Li, W., Liu, Y., and Jiang, Y. (2011). Numerical simulation of surface movement laws under different unconsolidated layers thickness. **Transactions of Nonferrous Metals Society of China**. 21: s599–s603.
- Désérable, D. (2002). A versatile two-dimensional cellular automata network for granular flow. **SIAM Journal on Applied Mathematics**. 62(4): 1414-36.
- Donnelly, L.J., Cruz, H.D.L., Asmar, I., Zapata, O., and Perez, J.D. (2001). The monitoring and prediction of mining subsidence in the Amaga, Angelopolis, Venecia and Bolombolo Regions, Antioquia, Colombia. **Engineering Geology**. 59(1–2): 103-114.
- Fattah, M.Y., Shlash, K.S., and Salim, N.M. (2013). Prediction of settlement trough induced by tunneling in cohesive ground. **Acta Geotechnica**. 8: 167–179.
- Guo, W., Hou, Q., and Zou, Y. (2011). Relationship between surface subsidence factor and mining depth of strip pillar mining. **Transactions of Nonferrous Metals Society of China**. 21: s594-s598.
- Helm, D.C. (1975). One-dimensional simulation of aquifer system compaction near pixley, California: 1. Constant parameters. **Water Resources Research**. 11(3): 465–478.

- Helm, D.C. (1976). One-dimensional simulation of aquifer system compaction near Pixley, California: 2. Dependent parameters. **Water Resources Research**. 12(3): 375–391.
- Holzer, T.L. (1981). Preconsolidation stress of aquifer systems in areas of induced land subsidence. **Water Resources Research**. 17(3): 693–704.
- Holzer, T.L. (1984). Ground failure induced by ground-water withdrawal from unconsolidated sediment. **Geological Society of America Reviews in Engineering Geology**. 6: 67–105.
- Islam, M.N., Siddika, A., Hossain, M.B., Rahman, A., and Asad, M. A. (2011). Effect of particle size on the shear strength behaviour of sands. **Australian Geomechanics**. 46(3): 75-86.
- Itasca. (2008a). **PFC2D–Particle Flow Code in 2 Dimensions, Version 4.0**. User Manual, Itasca Consulting Group Inc., Minneapolis, MN, USA.
- Jaeger, J.C., Cook, N.G.W., and Zimmerman, R.W. (2007). **Fundamentals of Rock Mechanics, (4th ed)**. Blackwell Publishing Ltd, Malden, MA. 475p.
- Jiang, M. and Yin, X. (2014). Influence of soil conditioning on ground deformation during longitudinal tunneling. **Comptes Rendus Mecanique**. 342: 189–197.
- Kim, D. and Ha, S. (2014). Effects of particle size on the shear behavior of coarse grained soils reinforced with geogrid. **Materials**. 7: 963–979.
- Kratszsch, H. (1983). **Mining Subsidence Engineering**. Springer-Verlag. Berlin, New York.
- Li, W., Liu, L., and Dai, L. (2010). Fuzzy probability measures (FPM) based non-symmetric membership function: Engineering examples of ground subsidence

- due to underground mining. **Applications of Artificial Intelligence**. 23(3): 420-431.
- Li, Z. and Wang, J. (2011). Accident investigation of mine subsidence with application of particle flow code. **Procedia Engineering**. 26: 1698–1704.
- Litwiniszyn, J. (1965). Some remarks on the stochastic theory of ground movement. **Rock Mechanics and Engineering Geology**. III/2: 69-75.
- Litwiniszyn, J. (1966). An application of the random walk argument to the mechanics of granular media. In **Rheology and Soil Mechanics Symposium, Grenoble** (pp. 82-89). International Union of Theoretical and Applied Mechanics, Berlin.
- Lofgren, B.E. (1968). Analysis of stresses causing land subsidence. **Geological Survey Professional Paper**. S600–B: B219–B225.
- Loganathan, N. and Poulos, H.G. (1998). Analytical prediction for tunneling-induced ground movements in clays. **Journal of Geotechnical and Geoenvironmental Engineering**. 124(9): 846-856.
- Martos, F. (1958). Concerning an approximate equation of the subsidence trough and its time factor. In **International Strata Control Congress** (pp. 191-205). Leipzig, Deutsche Akademie der Wissenschaften zu Berlin, Sektion für Bergbau.
- McCusker, T.G. (1982). Soft Ground Tunneling, Chapter 5. In Bickle, J.O. and Kuesel, T.R. (Eds). **Tunnel Engineering Handbook** (pp. 70–92). Van Nostrand Reinhold Company: New York.
- McNearny, R.L. and Barker, K.A. (1998). Numerical modeling of large-scale block cave physical models using PFC2D. **Mining Engineering**. 50(2): 72-75.

- Meguid, M.A., Saada, O., Nunes, M.A., and Mattar, J. (2008). Physical modeling of tunnels in soft ground: A review. **Tunnelling and Underground Space Technology**. 23: 185–198.
- Migliazza, M., Chiorboli, M., and Giani, G.P. (2009). Comparison of analytical method, 3D finite element model with experimental subsidence measurements resulting from the extension of the Milan underground. **Computers and Geotechnics**. 36(1-2): 113-124.
- Monsees, J.E. (1996). Soft Ground Tunneling, Chapter 6, 6th Ed. In O.B John., R.K. Thomas and H.K. Elwyn (Eds). **Tunnel Engineering Handbook** (pp. 97-121). Chapman & Hall: International Thomson Publishing Company, New York.
- Murayama, S., Shibata, T., Yamamoto, J. (1961). An experimental research on the subsidence of ground (I). In **Ann. of Disaster Preo. Res. Inst** (pp. 11-20). Kyoto Univ., Japanese.
- Nieland, J.D. (1991). **SALT_SUBSID: A PC-Based Subsidence Model**. Solution Mining Research Institute, Report No. 1991-2-SMRI, California, USA. 58pp.
- O'Reilly, M.P. and New, B.M. (1982). Settlements above tunnels in the UK-their magnitude and prediction. **Tunneling**. 82: 173–181.
- Oh, H. and Lee, S. (2010). Assessment of ground subsidence using GIS and the weights-of-evidence model. **Engineering Geology**. 115(1–2): 36-48.
- Papamichos, E., Vardoulakis, I., & Heil, L.K. (2001). Overburden modeling above a compacting reservoir using a trap door apparatus. **Physics and Chemistry of the Earth (A)**. 26(1-2): 69-74.

- Park, D. and Li, J. (2004). Subsidence Simulation Using Laser Optical Triangulation Distance Measurement Devices. In **Gulf Rocks 2004, the 6th North America Rock Mechanics Symposium (NARMS)** (pp. 6). Houston, Texas.
- Park, S.H., Adachi, T., Kimura, M., and Kishida, K. (1999). Trap door test using aluminum blocks. In **Proceedings of the 29th Symposium of Rock Mechanics. J.S.C.E.** (pp. 106–111). Japan.
- Peck, R.B. (1969). Deep excavations and tunneling in soft ground. In **Proceedings of the 7th international conference on soil mechanics and foundation engineering, State of the art volume** (pp. 225–290). Sociedad Mexicana de Mecánica de Suelos: Mexico.
- Poland, J.F. (1977). Land subsidence stopped by Artesian-head recovery, Santa Clara Valley, California. In **Proceedings of the Anaheim Symposium** (vol. 121, pp. 124–132). International Association of Hydrological Sciences.
- Powers, M.C. (1953). A new roundness scale for sedimentary particles. **Journal of Sedimentary Research.** 23(2): 117–119.
- Rankin, W. (1988). Ground movements resulting from urban tunneling. In **Prediction and effects, proceedings of 23rd conference of the engineering group of the geological society** (pp. 79–92). London Geological Society.
- Raymond, G.P. (1997). Shearing strength of soils. **Geotechnical Engineering.** 99–112.
- Reddish, D.J., 1989. The modeling of rock mass behaviour over large excavations using non-linear finite element techniques. **Min. Eng. Dep. Mag. Univ. Nottingham.** 41: 93–102.

- Ren, G. and Li, J. (2008). A study of angle of draw in mining subsidence using numerical modeling techniques. **Electronic Journal of Geotechnical Engineering**. 13: 1-14.
- Sakulnitichai, C., Pangpetch P. and Fuenkajorn, K. (2009). Physical model simulation of shallow openings in jointed rock mass under static and dynamic loads. In **Proceedings of the Second Thailand Symposium on Rock Mechanics** (pp. 147–160). Chonburi: Thailand.
- Scheidegger, A.E. (1966). Some implications of statistical transport theory in rock mechanics. **Pure and Applied Geophysics**. 65(III): 160-163.
- Schmidt, B. (1979). **Settlements and ground movements associated with tunneling in soil**. Ph.D. Thesis, University of Illinois.
- Shahriar, K., Amoushahi, S. and Arabzadeh, M. (2009). Prediction of surface subsidence due to inclined very shallow coal seam mining using FDM. In **Proceedings of the 2009 Coal Operators' Conference** (pp. 130–139). University of Wollongong: NSW.
- Shen, S.L., Xu, Y.S., and Hong, Z.S. (2006). Estimating of land subsidence based on groundwater flow model. **Marine Georesources and Geotechnology**. 24(2): 149–167.
- Singh, M.M. (1992). Mine subsidence. In H.L. Hartman (ed). **SME Mining Engineering Handbook** (pp. 938–971.). Society for Mining Metallurgy and Exploration: Inc. Littleton, Colorado.
- Tan, Z., Li, P., Yan, L., and Deng, K. (2009). Study of the method to calculate subsidence coefficient based on SVM. **Procedia Earth and Planetary Science**. 1(1): 970-976.

- Terzaghi, K. (1936). Stress distribution in dry and in saturated sand above a yielding trap-door. In **Proceedings of the International Conference on Soil Mechanics** (vol. 1, pp. 307–311). Harvard University Press: Cambridge, MA.
- Thongprapha, T., Fuenkajorn, K., and Daemen, J.J.K. (2015). Study of surface subsidence above an underground opening using a trap door apparatus. **Tunnelling and Underground Space Technology**. 46: 94–103.
- Vairaktaris, E. and Stavopoulou, M. (2013). Modeling of the three-dimensional subsidence diffusion-convection problem above a trapdoor. **International Journal for Numerical and Analytical Methods in Geomechanics**. 37(6): 551-576.
- Verruijt, A. and Booker, J.R. (1996). Surface settlements due to deformation of a tunnel in an elastic half plane. **Geotechnique**. 46(4): 753-756.
- Wang, J., Yu, H.S., Langston, P., and Fraige, F. (2011). Particle shape effects in discrete element modelling of cohesive angular particles. **Granular Matter**. 13: 1–12.
- Yao, X.L., Whittaker, B.N., and Reddish, D.J. (1991). Influence of overburden mass behavioural properties on subsidence limit characteristics. **Mining Science and Technology**. 13: 167–173.

BIOGRAPHY

Miss Thanittha Thongprapha was born on October 21, 1988 in Bangkok, Thailand. She received her Bachelor's Degree in Engineering (Geotechnology) from Suranaree University of Technology in 2010. For her post-graduate, she continued to study with Doctor of Philosophy Program in Geotechnology, Institute of Engineering, Suranaree university of Technology. During graduation, 2011-2014, she was a part time worker in position of research associate at the Geomechanics Research Unit, Institute of Engineering, Suranaree University of Technology.

